Deep–Sea Research I 203 (2024) 104198

Contents lists available at ScienceDirect

Deep-Sea Research Part I

journal homepage: www.elsevier.com/locate/dsri

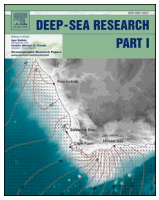

Multiscale spatial patterns and environmental drivers of seamount and island slope megafaunal assemblages along the Mozambique channel

Mélissa Hanafi-Portier [a,b,*], Sarah Samadi [b], Laure Corbari [b], Marion Boulard [a,c], Elda Miramontes [d], Pierrick Penven [e], Boris Leroy [f], Thibault Napoléon [g], Stéphan J. Jorry [h], Karine Olu [a]

[a] UMR 6197 BEEP, Biologie et Écologie des Écosystèmes Marins Profonds, Univ Brest, CNRS, Ifremer, Plouzané, France
[b] UMR 7205 ISYEB, Équipe "Explorations, Espèces et Spéciations", Muséum National d'Histoire Naturelle, Paris, France
[c] Department of Biology, Memorial University of Newfoundland, 45 Arctic Avenue, St John's, NL, A1C 5S7, Canada
[d] Faculty of Geosciences and MARUM-Center for Marine Environmental Sciences, University of Bremen, Bremen, Germany
[e] LOPS/UMR6523 (CNRS-IFREMER IRD-UBO), Laboratoire Océanographie Physique et Spatiale IUEM Technopole Brest Iroise Bâtiment D, Plouzané, France
[f] Unité Biologie des Organismes et Écosystèmes Aquatiques (BOREA, UMR 8067), Muséum National d'Histoire Naturelle, Sorbonne Université, Université de Caen Normandie, CNRS, IRD, Université des Antilles, Paris, France
[g] ISEN Yncréa Ouest, Laboratoire L@bisen, Équipe Vision-AD, Brest, France
[h] Geo-Ocean, Univ. Brest, CNRS, Ifremer, UMR 6538, Plouzané, France

ARTICLE INFO

Keywords:
Seamounts & island slopes
Bathyal megabenthic assemblages
Beta-diversity
Multiscale abiotic factors
Spatial & image analyses
Mozambique channel

ABSTRACT

Seamounts are vulnerable ecosystems targeted by fishing and potentially by future mineral exploitation. Their abundance, widespread distribution, and heterogeneity of faunal and abiotic components require integrated studies at multiscale to describe spatial patterns and identify environmental drivers needed by conservation plans. There is also a lack of knowledge on seamount benthic ecosystems in some regions, such as the Indian Ocean. These gaps, in the context of Marine Protected Areas establishment in the region, have motivated the present study focusing on the Mozambique Channel Eparses islands and flat top seamounts, along a 10-degree latitude gradient. These structures are characterized by complex volcanic and carbonate geomorphologies at multiscale and are distributed along a highly dynamic turbulent ocean circulation area with large anticyclonic eddies. For the first time, we analysed, from seabed image transects obtained by towed-camera on four seamounts, and two volcanic islands - Bassas da India and Mayotte - external slopes, and from multiscale environmental data, how benthic communities respond to this high habitat heterogeneity at regional, and local scales. This study reveals high discrepancies of benthic megafauna richness, density, and beta diversity among seamounts and among slopes of the same islands. Moreover, at similar latitude, seamounts display higher densities than island slopes. The highest densities found on a seamount of the Glorieuses archipelago are explained by strong currents and flat homogeneous geomorphology. Except on this seamount, the beta diversity is high, despite the quite limited depth range explored (84–734 m) and is the highest on island slopes and Hall Bank, driven by the diversity and hardness of the substrate. Beta diversity is mainly due to taxa turnover, with high contribution of the habitat-forming sponges and cnidarians, together with a few mobile taxa. We identified from biogeographic network analysis 12 dominant faunal assemblages, displaying a patchy distribution, with variability in composition both among and within sites. Currents and primary productivity explain ~15% of the observed assemblage structure along the channel, while geomorphology (km scale), topography (60–500 m scale) and substrate (60-m units) explain together 24% of the faunal spatial patterns. Analysis of spatial structures along island slopes detected some small (100–200 m), medium (~1 km) and large scale (~2–6 km) megabenthic community structures, partly explained by topography, substrate, depth, and slope. Despite limited taxonomic identifications for this poorly sampled area, this study reveals an outstanding heterogeneity of megabenthic assemblages at multispatial scales in the Mozambique Channel seamounts and island slopes, in response to the complex hydrography and geology of the area. Further characterization of environmental drivers with greater focus at local scales including hydrographic variables are therefore needed to improve predictions of suitable habitats of vulnerable marine ecosystems.

* Corresponding author. UMR 6197 BEEP, Biologie et Écologie des Écosystèmes Marins Profonds, Univ Brest, CNRS, Ifremer, Plouzané, France.
E-mail address: hanafimelissa@gmail.com (M. Hanafi-Portier).

https://doi.org/10.1016/j.dsr.2023.104198
Received 29 March 2023; Received in revised form 12 November 2023; Accepted 15 November 2023
Available online 19 November 2023

1. Introduction

Seamounts are isolated topographic features of geological origin that rise at least 1000 m above seafloor (Rogers, 2018). When emerging above the sea surface, these topographies are defined as oceanic islands, whose nearshore features are more subject to nutrient input and terrigenous runoff from the land (Staudigel and Clague, 2010). Interaction of oceanic circulation with seamounts generates eddies formation and other circulation cells such as internal waves and Taylor column formation (i.e., doming structure above the seamount) (White et al., 2007; Clark et al., 2010). These rectified flows potentially enhance particulate mixing, and in addition to the trap of vertically migrating zooplankton, would contribute to support a highly productive system, especially of dense aggregation of benthopelagic and demersal fish (Morato et al., 2008, 2010; Clark et al., 2010). For this reason, seamounts are targeted by commercial fisheries (Morato and Clark, 2007). In addition, some of these structures are covered by cobalt-rich ferromanganese surface deposits which are of potential economic interest for seabed mining of their rare metals (Hein et al., 2010). Increased hydrodynamic flow, prevalence of hard substrata and high concentration of nutrients and preys foster the settlement of epibenthic suspension feeders (Genin et al., 1986). These megabenthic animals (i.e., benthic megafauna; animals of sufficient size to be observable from images, ~2 cm (Grassle et al., 1975)) are commonly observed over seamounts (e.g., Porifera, Actiniaria, Octocorallia, Brachiopoda, Crinoidea) (Rogers, 2018). Some of these organisms can form more or less dense biological aggregates (e.g., cnidarians, sponges) - that can host a diversified associated fauna composed mainly of small benthic invertebrates (e.g., crinoids, brittle stars, squat lobsters and other small decapods, mollusks) (Buhl-Mortensen et al., 2010). These large habitat-forming invertebrates are long-lived and slow-growing and threatened by deep-sea commercial trawling leading to use them as VME indicator taxa (Althaus et al., 2009; Baco et al., 2020). Their ecological importance associated with their poor resilience contribute to the vulnerability of benthic populations on seamounts.

Although the estimates of the number of these underwater structures range from 150,000 to 25 million worldwide depending on seamount definition (*sensus stricto* > 1000 m or *sensus lato* > 100 m) and the method used to make the estimation (Rogers, 2018), fewer than 0.4%–4% have been sampled to date (Kvile et al., 2014), mainly in the Atlantic and Pacific regions (Clark et al., 2010; Rowden et al., 2010a). Consequently, our knowledge on the structure of seamount benthic communities and their driving factors is still limited. Moreover, seamounts occur across a wide variety of latitudes and depth ranges and have diverse morphologies. Benthic communities are thus affected by multiple environmental forcings, whose influence depends on the spatial scale considered. Furthermore, the benthic composition of seamounts depends on the biological province in which they lie (Watling et al., 2013; Watling and Lapointe, 2022; Maureaud et al., 2023).

Megabenthic assemblages on seamounts vary from patchy distribution along a mosaic of habitats within a single seamount to overall change among seamounts over geographic distance (Clark et al., 2010; Rogers, 2018). The controlling factors of this spatial heterogeneity have been explored in several case studies, focusing on one or a few seamounts, in a few regions of the world. Within the different studied regions, the benthic megafauna communities of the set of surveyed seamounts were shown to be structured by surface primary productivity (Clark and Bowden, 2015; Bridges et al., 2022), temperature and oxygen concentration, and particulate organic carbon concentration (O'Hara et al., 2010), latitudinal gradient (Williams et al., 2011; Morgan et al., 2015), distance from the coast (O'Hara et al., 2010), as well as depth gradients (Williams et al., 2011; Schlacher et al., 2014; Boschen et al., 2015; Clark and Bowden, 2015; Lapointe et al., 2020). The role of bathymetric gradients is related to the different water masses that cross the seamounts, which are themselves factors that structure the communities (Auscavitch et al., 2020a; Lapointe et al., 2020; Bridges et al., 2022).

Other studies explored in more detail the factors acting at a local scale. For example, some studies showed that on a single seamount scale, depth-related factors (McClain et al., 2010; Long and Baco, 2014; Du Preez et al., 2016; Ramos et al., 2016; Victorero et al., 2018; Morgan et al., 2019) and water masses (Victorero et al., 2018) structured the distribution of the benthic megafauna. Currents, although very rarely tested, seem to explain the varying compositions of benthic assemblages on the different seamount flanks (Morgan et al., 2019). The geomorphology of the different seamounts, resulting from their own geological history, generates a variety of landforms (ripples, flanks, summits) and substrates (e.g., lava lobe, massive boulder, bedrock, small pebbles) displaying seafloor heterogeneity over different spatial scales, as well as different microtopography. These seafloor parameters also appear in different studies as structuring the communities both at the seamount scale and among seamounts (Sautya et al., 2011; de la Torriente et al., 2018; Victorero et al., 2018; Shen et al., 2021). An important source of heterogeneity in the communities comes from the presence of biogenic habitats, including corals and sponges. Many studies underlined the heterogeneity in the distribution of these habitat-forming organisms with areas presenting scattered animals to dense plurispecific aggregates (Morgan et al., 2015; Auscavitch et al., 2020b; Baco et al., 2020). Some studies showed that faunal densities can moreover change through geological time scale (Bo et al., 2020).

In summary, previous studies revealed that multiple controlling factors, both physical and biological, operate at various spatial scales to drive the heterogeneity in benthic communities. To better understand the spatial pattern of seamount benthic assemblages, it is necessary to consider an integrative approach, at various spatial scales, comparison among different seamounts and at the seamount scale, combined with the whole set of environmental parameters under hypotheses, with biological data obtained by the same data acquisition methods. Indeed, most of the previous studies have either focused on a single seamount (usually using remotely operated vehicle (ROV) and imagery data) (e.g., Piepenburg and Müller, 2004; Lundsten et al., 2006; McClain et al., 2009; Starr et al., 2012; Narayanaswamy et al., 2013; Long and Baco, 2014; Davies et al., 2015; Henry et al., 2015; Du Preez et al., 2016; Ramos et al., 2016; de la Torriente et al., 2018; Victorero et al., 2018; Morgan et al., 2019; Shen et al., 2021), or have integrated several seamounts of a given region, most of the time based on dredge and trawl data (e.g., O'Hara, 2007; O'Hara et al., 2008; Tittensor et al., 2009; Miller et al., 2010; O'Hara and Tittensor, 2010; Rowden et al., 2010c; Williams et al., 2011; Braga-Henriques et al., 2013; Pante et al., 2015; Miyamoto et al., 2017; Miyamoto and Kiyota, 2017). On the one hand, studies based on towed gear sampling provide accurate taxonomic data and allow a qualitative description of large-scale biodiversity patterns (bioregions), endemism (O'Hara, 2008; MacPherson et al., 2010) and connectivity (Cho and Shank, 2010; Miller and Gunasekera, 2017) on seamounts. However, these data neither allow the quantification and the description of community structure at fine spatial scales nor integration of fine resolution environmental data. On the other hand, studies of seamount megabenthic communities relying on images are usually conducted with a morphospecific (morphotype) approach (e.g., Piepenburg and Müller, 2004; Victorero et al., 2018; Mecho et al., 2019; Bridges et al., 2021; Puerta et al., 2022; Stratmann et al., 2022), for which taxonomic data are not very robust and not comparable between studies (Hanafi-Portier et al., 2021). Furthermore, many oceanic regions of the world remained largely undersampled, such as the Indian Ocean (Kvile et al., 2014) where only one study has been carried out on seamount communities to our knowledge (Sautya et al., 2011).

The northern part of the Mozambique Channel (western Indian Ocean) is a second hotspot of tropical marine biodiversity after the coral triangle in the Pacific and displays a high diversity of reef corals (Obura et al., 2012). The exploration of the deep-sea habitats of this region is mainly limited to the north of the Channel (e.g., Thomassin, 1977; Castelin et al., 2017). We visually explored for the first time between

2014 and 2017 several geomorphologic structures along a 10° latitudinal gradient within the channel. Explorations focused on the seamount summits and upper slopes, as well as on island slope terraces, in a bathyal range (370–1180 m). These structures show a diversity of morphologies and substrates, inherited from their volcanic origin and their complex geological evolution (Audru et al., 2006; Courgeon et al., 2016, 2017). Among them, the Mayotte Island and the Glorieuses archipelago are both part of marine protected areas, the former under the management of the French Biodiversity Office (Office français de la biodiversité; OFB), and the latter under the management of the French Southern and Antarctic Territories (Terres Australes et Antarctiques Françaises; TAAF).

Based on the image dataset combined with faunal sampling (by towed gears), and on environmental data collected at multiscale (~1400 km-60 m) from ocean databases (chlorophyll), current modelling, high resolution bathymetric data and image analyses (substrata), we aimed to: **(1)** compare community metrics (density, taxonomic richness and beta diversity) of several seamounts and island slopes and search for environmental driving forces explaining these differences, **(2)** describe spatial distribution patterns of megabenthic communities among and within sites, and assess the influence of multiscale environmental factors, and finally, **(3)** differentiate scales of spatial structures and their interrelationships with abiotic factors at local scale, along the slopes of Mayotte and Bassas da India Island.

2. Materials and methods

2.1. Study area

The Mozambique Channel is located in the western Indian Ocean, between the East African Margin and the island of Madagascar, (400–900 km wide, about 1700 km long) between S10° and S25° latitude (Fig. 1A). The region is characterized by a unique and complex hydrographic system, rich in mesoscale eddies, up to 300 km in diameter. These eddies are generated north of the channel at a frequency of 6–8 per year and flow southwards at a speed of ~4.5 km per day (de Ruijter et al., 2004). In contact with the continental shelves of the Mozambique and Madagascar margins, these eddies affect the variability of primary productivity, which is increased at their center, and can reach the ocean floor to a depth of 2000 m (de Ruijter et al., 2002). The presence of coastal upwelling, particularly along the Madagascar coast, is also a source of particulate input to the open sea (Marsac et al., 2014). The north of the channel is dominated by a strong westerly current (Northeast Madagascar Current, NEMC) which splits into two branches at the intersection with the Davie Ridge and the East African coast, flowing in a southward and northward direction respectively (Fig. 1A) (Collins et al., 2016). The Mozambique Channel consists of five main water masses (from 0 to 1500 m depth). From the north, the NEMC transports salty Tropical Surface Water (TSW), Subtropical Surface Water (STSW) and South Indian Central Water (SICW) to a depth of about 600 m. In the intermediate water, oxygen-poor Red Sea Water (RSW) (~900–1200 m) enters the channel from the north along the East African coast, and circulates southwards, notably carried into the core of mesoscale eddies. To the south of the channel, Intermediate Antarctic Water (AAIW) (800–1500 m), is transported northwards by the Mozambique undercurrent along the Mozambique coast (de Ruijter et al., 2004; Collins et al., 2016; Charles et al., 2020). The region exhibits seasonal variation in chlorophyll *a* (Chla) concentrations, with the highest levels in winter due to wind regimes and mesoscale eddies that cross the channel, and low sea surface Chla concentrations (<0.2 mg/m^3), constituting an oligotrophic region (Malauene et al., 2014). Chla concentrations do not exceed 1 mg/m^3 in deep water in the channel (average concentration of 0.15 mg/m^3) (Tew-Kai and Marsac, 2009). Primary production rates are twice as high in the south of the channel in winter compared to the north. The main differences in physical forcing between the northern, central, and southern parts of the channel are due to the intense mesoscale eddies in the central and southern parts incorporating a non-seasonal signal, while the northern circulation is predominantly monsoonal (Langa, 2021). The Mozambique Channel hosts various seamounts and carbonate platforms, resulting from intense volcanic and tectonic activities originating from the emergence of the channel 180 million years ago. The Davie Ridge was formed from these activities; it extends from the East African margin to Madagascar (9°S-23°S) and consists of various seamounts, notably the Sakalaves platform (17–19°S) (Fig. 1A) (Courgeon et al., 2018). The southern part of the channel hosts two guyots (Hall and Jaguar banks) as well as a modern atoll (Bassas da India), which lies on a 12-km wide drowned terrace (Courgeon et al., 2017). To the north, the channel hosts the Comoros archipelago, comprising in the eastern part Mayotte Island (Fig. 1A). Further north, a drowned carbonate platform lies off the Glorieuses Islands (Courgeon et al., 2016). These reliefs, formed by volcanic activity, were colonized by shallow-water reefs, before subsiding and being eroded at depth. For some features (Jaguar, Hall Bank, Bassas da India), a reactivation of volcanism was accompanied by tectonic deformations, resulting in highly heterogeneous substrates, ranging from fractured volcanic outcrops and lava flow fields to large areas of sand dunes (Courgeon et al., 2017; Miramontes et al., 2019a). For Glorieuses, the geological evolution has resulted in the formation of carbonate terraces covered with sandy deposits shed from the island (Courgeon et al., 2016, 2017; Jorry et al., 2020). We will refer to the term seamount for all the topographic features studied (seamounts, atolls, or terraces, guyots and carbonate platforms), except for the island slopes (Bassas da India, Mayotte). These volcanic islands have a similar origin, and the terraces explored along their slopes can be compared to seamount summits, as they are hypothesized to have been eroded during aerial phases before subsidence (Audru et al., 2006). The island of Mayotte is composed of a barrier reef that encloses a lagoon (1100 km^2). The island's outer slopes are characterized by a complexity of geomorphologies and substrates, and are composed of a network of canyons, vast plateaus/terraces, cliffs, volcanic cones, and rugged areas (Audru et al., 2006).

2.2. Data acquisition

2.2.1. Study sites and image data

The data were obtained from the cruises PAMELA-MOZ01 (Olu, 2014) onboard the research vessel (R/V) *L'Atalante* and PAMELA-MOZ04 (Jouet and Deville, 2015) onboard the R/V *Le Pourquoi Pas?* These cruises were part of the PAMELA (PAssive Margin Exploration LAboratories) project (Bourillet et al., 2013) and explored four seamounts along the Mozambique Channel, from North to South: a carbonate platform in the Glorieuses Archipelago, the Sakalaves mounds along the Davie Ridge, Jaguar, and Hall Bank, as well as a terrace in Bassas da India closely located to the latter (Fig. 1A, B, D-G). The BIOMAGLO (BIOdiversité MAyotte-GLOrieuses) cruise (Corbari et al., 2017), onboard the R/V *L'Antea*, completed the image dataset with an exploration of the outer slopes of Mayotte Island. Three slope orientations were selected for the study – North, East, and West – (Fig. 1C). The western and northern slopes are characterized by the presence of terraces located at similar depths to the seamount summits. A total of nine camera transects were analysed for this study (details in Table 1). The images were captured using a towed-camera system (SCAMPI, IFREMER dev.), with an HD camera (NIKON D700, focal length 18 mm, resolution 4256 × 2832 pixels), in a vertical position, at a speed of about 0.5 m/s, at intervals of 30 s (except for Glorieuses, about 15 s), and at an average altitude of 2.5–3 m above the seabed. The images were georeferenced using the vessel positioning system processed with the ADELIE application (French oceanographic fleet) developed at IFREMER and implemented using the ArcGIS V10.3 software.

2.2.2. Environmental data

We used bathymetry and acoustic reflectivity data acquired by the

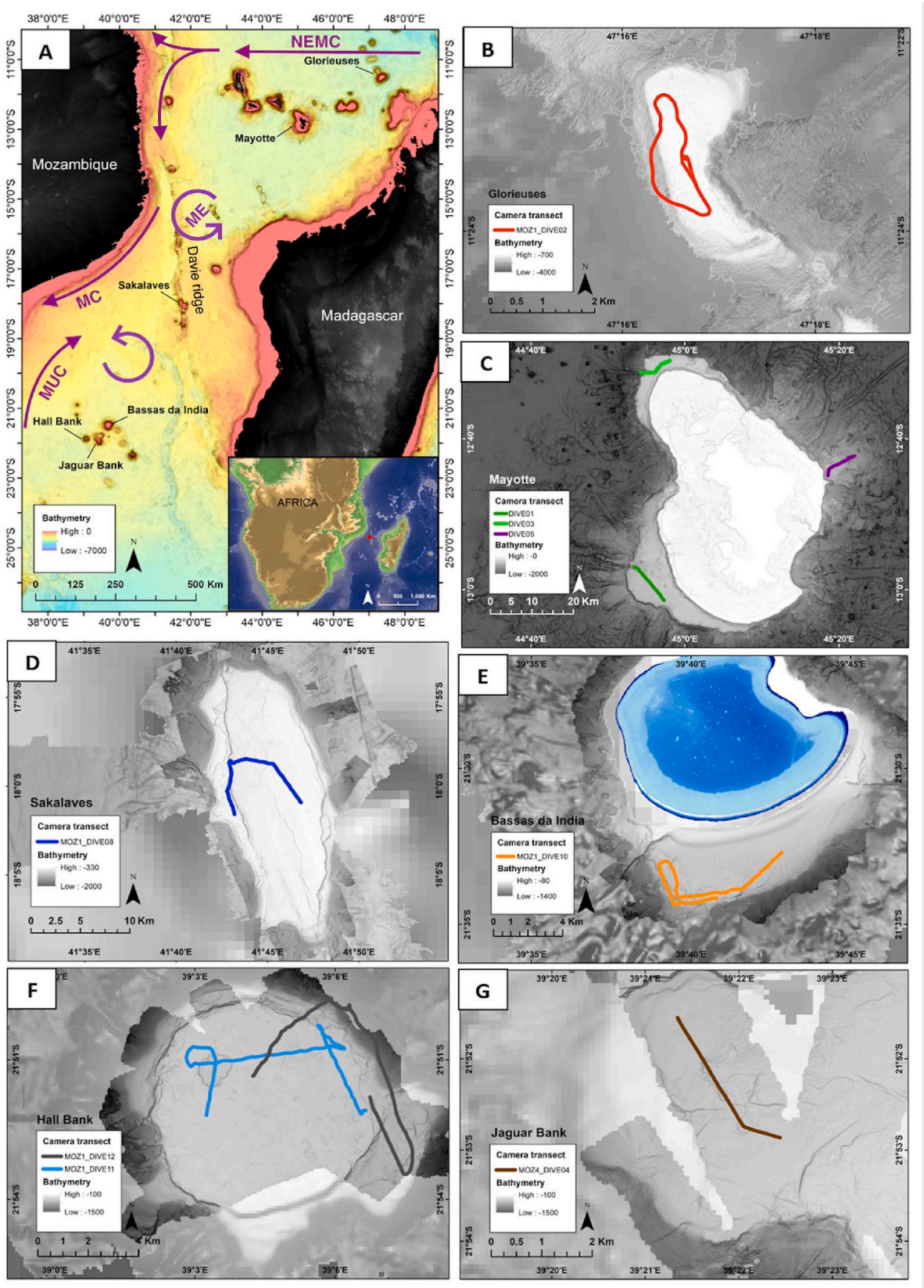

Fig. 1. **(A)** Location of the different seamounts and islands explored in the Mozambique Channel with the main currents flowing across these features (NEMC: Northeast Madagascar Current, MC: Mozambique Current, MUC: Mozambique Undercurrent, ME: Mozambique Eddies (from Collins et al., 2016; Charles et al., 2020), and specific maps of each towed camera transect on seamounts and island slopes: **(B)** Glorieuses, **(C)** Mayotte Island slopes, **(D)** Sakalaves platform, **(E)** Bassas da India Island, **(F)** Hall Bank, **(G)** Jaguar Bank. (format: 2-column image).

Table 1
Summary of sampling effort, location, and depth for the nine towed camera transects.

Cruise	Site	Geomorphology	Camera transect	Depth range (m)	Number of images	Number of analysed images	Transect length (km)	Latitude (start-end transect)	Longitude (start-end transect)	Number of 200 m^2 polygon (sampling unit)
Biomaglo	Mayotte, West slope	Island slope (terrace)	DIVE01	654–888	900	877	11	−13.02/-12.95	44.95/44.89	191
	Mayotte, North slope	Island slope (terrace)	DIVE03	449–1183	1101	985	8	−12.49/-12.52	44.97/44.90	121
	Mayotte, East slope	Island slope	DIVE05	492–1117	938	899	8.5	−12.75/-12.70	45.30/45.37	149
Pamela MOZ01	Glorieuses	Carbonate platform	MOZ1 DIVE02	724–883	1155	851	6	−11.39/-11.38	47.28/42.28	106
	Sakalaves	Platform and escarpment	MOZ1 DIVE08	368–482	1361	1296	15	−18.02/-18.01	41.72/41.78	268
	Bassas da India	Island slope (terrace and upper slope)	MOZ1 DIVE10	453–623	1123	1021	14	−21.54/-21.57	39.71/39.68	248
	Hall (summit)	Bank summit	MOZ1 DIVE11	456–540	1170	1126	16	−21.87/-21.85	39.05/39.07	279
	Hall (summit-slope)	Bank summit, terrace upper slope	MOZ1 DIVE12	480–903	1050	936	16	−21.86/-21.86	39.11/39.07	256
Pamela MOZ04	Jaguar	Bank summit	MOZ4 DIVE04	456–549	926	439	3	−21.88/-21.86	39.37/39.36	58

BATHYMAY (BATHYmetry MAYotte) cruise for the Mayotte island slopes (Audru et al., 2006). For all the other sites, multibeam bathymetric data were acquired during the PTOLEMEE (PasT glObaL changEs in the MozambiquE channEl) (Jorry, 2014) and PAMELA-MOZ01 (Olu, 2014) cruises with a multibeam echosounder (Kongsberg EM122 for the deepest areas and EM710 for the shallowest areas) (Courgeon et al., 2016). CTD (temperature, salinity, pressure) and oxygen data were acquired during the SCAMPI dives from CTD SBE19 and optode (microcat) sensors mounted on the camera frame. The temperature sensor did not work for the northern slope of Mayotte, nor did the oxygen sensor for the dive on the Sakalaves platform.

2.3. Taxonomic data processing from images

We annotated 9724 images using BIIGLE 2.0 (Langenkämper et al., 2017). Details of the method for identifying taxa in images are described in Hanafi-Portier et al. (2021). The taxonomic identification is based on objective criteria (morphological characters of the taxon) and contextual criteria (knowledge of similar species collected in the region and their habitat). The characters that can be observed on images are not equally informative among the taxonomic groups. We selected a taxonomic rank for each taxon as follows: (1) to avoid taxonomic rank nesting (e.g., in the family Nematocarcinidae most individuals were identified at the genus level *Nematocarcinus*, we thus selected the genus rank and removed the few individuals identified only at the family level except if we are certain that they do not belong to the genus *Nematocarcinus*), (2) to compromise between abundance (number of individuals identified per rank) and diversity (number of taxa included in the dataset). Thus, different identification ranks were achieved in the dataset, with low taxonomic ranks (genus for echinoids and asteroids, morphospecies/species for decapods) and higher ranks (Phylum for brachiopods and annelids, Class for poriferans, molluscs and other echinoderms, Order for fish and cnidarians). Furthermore, we did not consider the individuals in the dataset that were identifiable only at high rank (e.g., Actinopterygii spp., Porifera spp., Cnidaria spp., Asteroidea spp.), representing 16,7% of the total number of individuals. We exported the annotations from BIIGLE, then we compiled the faunal data at the taxonomic ranks selected for the analysis, to obtain a faunal abundance matrix (list of the taxonomic composition in Supplem. mat. 1).

To obtain robust ecological signals accounting for the low faunal count per image in our study area, we aggregated the abundance per image into 200 m^2 (~60 m linear) sample units (i.e., polygons) defined spatially from the navigation of the camera and its speed, using the ADELIE software (internal dev. IFREMER; ArcGIS 10.7 plugin). The 200 m^2 area was an optimum surface allowing to obtain at least three images per polygon for most of them, while having a compromise between fauna density and habitat heterogeneity. The slightly variable speed of the towed camera and the removal of poor-quality images (1294, ~13% of the total dataset) from the dataset meant that we observed a variable number of images per polygon (from four to eight in average). We therefore weighted the summed abundances in each polygon by the number of images in the polygon, and then standardized the densities by the area of the polygon. We deleted all polygons with less than two images and kept only polygons ranging from 170 to 200 m^2. We finally kept 8430 images out of a total of 9724 and we kept 1676 polygons out of a total of 1767 for the analyses (Table 1).

2.4. Environmental data processing

To consider the influence of oceanic circulation, eddies, and related particulate export of the deep-water layers on the communities, average modelled current velocity, and variability (standard deviation) data were obtained for three depth layers (0–50 m, 50–200 m, 300–650 m). The current velocity simulation (MOZ36) was based on the CROCO ocean model (Coastal and Regional Ocean COmmunity model; http://www.croco-ocean.org/). CROCO, an evolution of the ROMS ocean model (Shchepetkin and McWilliams, 2005), solved here the primitive equations for the ocean circulation following the hydrostatic and Bousinesq approximations and using a topographic following vertical coordinate. We defined 60 vertical levels. To reach a horizontal resolution of 1/36° (2.9 km at 20°S), we used three levels of nested grids communicating between each other, based on the AGRIF library (Debreu et al., 2012). The bottom topography was derived from the Global Earth Bathymetric Chart of the Oceans (GEBCO, 2014) dataset (Weatherall et al., 2015). A smoothing was applied locally to prevent numerical imprecision. The surface boundary conditions were based on a bulk formulation (Fairall et al., 1996), using the daily ERA-INTERIM atmospheric reanalysis (Dee et al., 2011). The lateral open boundary conditions were forced by monthly average outputs from the GLORYS 1/4° oceanic reanalysis (Ferry et al., 2012). The model was run for the 1993–2014 period after a spin-up of 2 years. This simulation allowed us to show the influence of Mozambique channel rings on bottom currents and morphology (Miramontes et al., 2019b). We exported the monthly

satellite data of daily mean surface Chla concentrations (4 km × 4 km resolution), from the AquaMODIS database. We considered seven years of integration for the Hall, Bassas da India and Sakalaves sites (2007–2014), eight years for Jaguar (2007–2015) and ten years for Mayotte and Glorieuses (2007–2017), depending on the dates of data acquisition for the different cruises and sites. We calculated the winter and summer climatologies, to consider the contrasted differences in primary productivity of the region (Tew-Kai and Marsac, 2009), as well as the minimum, maximum, average Chla (from seven to ten years of monitoring), and the average intra-annual and inter-annual variability, to test if extreme values and Chla variability influence communities' structure along the Mozambique Channel. CTD (temperature, salinity) and oxygen data from SCAMPI dives were georeferenced in ArcGIS to calibrate the time step of acquisition at each frame/image (CTD profile in Supplem. mat. 2).

High resolution bathymetry (Digital Terrain Model – DTM) and acoustic imagery were processed from multibeam echosounder data. DTM resolution was 10 m for the PAMELA project data (Charline Guerin, IFREMER Marine Geosciences lab), and 20 m on the explored areas of Mayotte (Audru et al., 2006; SHOM data). We quantified the terrain variability using bathymetric-derived indices with the Benthic Terrain Modeler (BTM) plugin in ArcGIS V10.7 (Walbridge et al., 2018). The scale of the measured indexes was therefore dependent on the DTM resolution. We considered the explanatory seafloor variables considered relevant in the literature for understanding the structure of megabenthic communities (Wilson et al., 2007). The Bottom Position Index (BPI) was calculated to measure the average differences in bottom elevation relative to a reference point successively within a moving window. It was calculated at fine (30, 60, 90 m) and large (120, 250, 500 m) scales to capture the smallest structures (faults, ripples) to the largest ones (craters, slope breaks, escarpments) on the different features. We also measured the following variables from a moving window of 3 × 3 cells, conditioned by the BTM plugin (i.e., 30 m scale considering 10 m resolution x 3 cells = 30 m, except for Mayotte at 60 m): longitudinal, transverse and total curvature; aspect converted to eastness and northness (bounded between −1 and 1) from the cosine and sine of the aspect angle; bottom roughness from an Arc Chord method, to obtain a roughness value independently of the slope value (Du Preez et al., 2016), as well as the slope. We then calculated the statistics – mean, minimum, maximum and standard deviation – of the terrain variables, the Chla, the current, the oxygen and the temperature per polygon in R.

We defined four geomorphological classes to characterize structures greater than one km-scale on each site: (1) a volcanic geomorphology, with volcanic reliefs such as lava flows, lobes, boulders, or blocks, (2) a carbonate geomorphology, relatively flat, forming slabs of rather homogeneous carbonate rock, with a few potential fractures. This geomorphology can also reflect discontinuous carbonate reliefs (eastern slope of Mayotte Island), or large blocks of carbonate rock or walls (western slope of Mayotte), (3) a sedimentary geomorphology, composed of large sandy areas, sometimes with dunes and ripples, (4) a mixed geomorphology, with a mixture of volcanic relief and carbonate substratum, and a sedimentary area. The classification relied on the interpretation of the bottom reflectivity, and by overlaying slope and bathymetry data in ArcGIS to distinguish volcanic substratum (mainly lobe shape) from carbonate one (homogeneous, fractured). We then ground-truthed the classes by observing a set of 30 *in situ* images for each class and transect (catalogue of geomorphological classes in Supplem. mat. 3).

We characterized and semi-quantified the substrate composition from a machine learning algorithm which pre-classified the substrate type in the images. For the algorithm, we defined five substrate classes: volcanic rock, carbonate slab, sand (fine sediment), gravel (coarse sediment), and biogenic debris (coarse discontinuous substrates composed of e.g., coral rubbles, shells). False classifications due to high substrate heterogeneity and of image brightness were manually corrected. However, as it was too time-consuming to delineate substrate classes manually on all images, we defined substrate facies and distinguished primary from secondary and mixed substrates using manual observation of >50% or <50% and 50-50 image coverage respectively using a home-made substrate catalogue for the reference leading in the end to possible combinations of 17 substrate facies from the five initial classes (Supplem. mat 4). For ease of analyses and interpretations, we grouped substrate facies into nine categories (i.e., 100% sediment, 100% carbonate rock, 100% volcanic rock, 100% gravel, 100% biogenic, mixed rock, mixed carbonate-sediment, mixed volcanic-sediment, mixed (sediment, volcanic, carbonate). The occurrences per image were then used to calculate (1) substrate frequencies/polygon, (2) substrate diversity/polygon (Shannon Weaver, exponential component) (details in Supplem. mat. 4). We calculated a hardness index/polygon, by applying a substrate hardness score between 1 and 6 (e.g., from 1: 100% soft to 6: 100% hard) to the 17 substrate facies (details in Supplem. mat. 4). The summary of the environmental variables and abbreviations are available in Supplem. mat. 5.

2.5. Statistical analyses

2.5.1. Community structure

We performed statistical analyses using R software (V4.1.2) (R Core Team, 2021) and made graphical representations with the ggplot2 package (Wickham et al., 2016).

For all analyses, faunal densities were quadratic-root-transformed to reduce the weight of highly abundant taxa compared to intermediate to poorly abundant taxa. This transformation affects large values more strongly than small values and thus reduces the skewness of the dataset (Legendre and Legendre, 2012). A Hellinger transformation of the data was also applied to densities ('vegan' package (Oksanen et al., 2020), *decostand()* function). This transformation is recommended for community-type datasets in ecology that usually contain many zeros, as it gives little weight to variables with low values and double absences (Legendre and Gallagher, 2001).

We assessed taxonomic richness among sites, using sample-based (i.e., polygons) rarefaction curves on faunal presence/absence data ('iNEXT' package (Hsieh et al., 2020), *iNEXT()* function). The taxonomic richness rarefaction for the smallest sampling effort (n = 58 polygons) and extrapolation for a sampling effort close to the asymptote of each curve (n = 400 polygons) were obtained with the 'iNEXT' package, *estimateD()* function. We quantified a total beta diversity (BD) for each transect and two sub-indices as well: LCBD (Local Contribution to Beta Diversity) and SCBD (Species Contribution to Beta Diversity) with the 'adespatial' package (Dray et al., 2022), *beta. div()* function. LCBD values reflect the level of uniqueness of each sampling unit, i.e., polygons with high LCBD represent sites where the community composition is unique and tends to generate variability along the transect. We tested significant LCBDs by a permutation test ($p < 0.05$, n = 999). The SCBD coefficients represent the level of variation of each individual taxon in the study area considered. Thus, a taxon with a high SCBD value will contribute more strongly to the BD (Legendre and De Cáceres, 2013). We performed a partition of the BD into the 'replacement' and 'abundance difference' components, for the latter on Hellinger-transformed densities, using the % difference coefficient, from the Podani indices family ('adespatial' package, *beta. div.comp()* function). Replacement (also called turnover) reflects the trend for taxa to replace each other along a sufficiently long gradient, while abundance difference reflects that one community may include more abundant taxa than another (Legendre, 2014). We compared densities among the nine seamounts/island slopes using a Kruskall-Wallis test for significance of density differences ('vegan' package, *kruskal. test()* function), and a post-hoc test of pairwise comparisons between the different groups with a Bonferroni correction applied for multiple testing (*pairwise.wilcox.test()* function).

We delineated megabenthic assemblages using biogeographic networks clustering, as an alternative approach to distance-based clustering (e.g., beta-diversity), recently introduced in biogeography (Vilhena and

Antonelli, 2015). This approach is usually used to delineate bioregions. It consists in creating a bipartite site-species network. When a species is sampled in a site, a link is drawn between the taxon and the site. Thus, links are only drawn between sites and taxa - no site-site or taxon-taxon links. We weighted the site-taxa links with the sampled abundance of taxa in sites. Upon the weighted bipartite site-taxa network, we applied the community detection algorithm Map Equation because it has been recommended in biogeographical studies (Edler et al., 2016; Rojas et al., 2017; Leroy et al., 2019), and it can detect the hierarchical structure of communities. Clusters detected by Map Equation with link weights have a high-intra group connectivity of links with high weights, and low inter-group connectivity of links with low weights. In other words, the algorithm groups together sites which share taxa in similarly high densities; different clusters have distinct compositions in terms of the most abundant taxa. We ran map equation with 100 trials to find the optimal partition in the dataset. We used the R 'biogeonetworks' package to perform the clustering procedure (Leroy (2022), step-by-step code available at https://github.com/Farewe/biogeonetworks). The main assets of the network-based approach over distance-based approaches are (1) the identity of species is preserved throughout the procedure, i.e., they are not abstracted into distances; (2) the clustering algorithm assigns species to clusters, which facilitates understanding the structure of clusters and relationships among clusters; (3) it is robust to differences in sampling intensities, which makes the removal of sites with low numbers of species unnecessary (Leroy et al., 2019). For each cluster, we quantified the indicator values of taxa, their specificity and fidelity within their assemblages, with the 'labdsv' package (Roberts, 2019), *indval()* function. Specificity is the relative abundance of the species across clusters (total abundance of the species within the cluster/the species total abundance). Fidelity is the relative frequency of the taxon in each cluster (number of sites where the species is present/number of sites in the cluster). The indicator value IndVal is the product of Fidelity * Specificity and allows the identification of characteristic taxa for a cluster (Dufrêne and Legendre, 1997; Roberts, 2019).

2.5.2. Role of environmental factors

We tested the environmental drivers of richness, density and BD differences among sites using simple and multiple regression models. For the density and beta diversity response variables (continuous quantitative), we used the *lm()* function of the 'stats' package (R Core Team, 2021). For the richness (discrete quantitative), we used generalized linear regression models, following a Poisson distribution, with the *glm()* function of the 'stats' package.

We tested the environmental drivers of the assemblages composition using a redundancy analysis (RDA), with the 'vegan' package, *rda()* function. Since this analysis is sensitive to collinearities between variables, we first evaluated the collinearities between environmental variables using Pearson pairwise correlations and removed the variables with high collinearities (Pearson $r > 0.85$) (See Supplem. mat. 5 for the list of variables used in the RDA and co-linear ones). We tested the model, variables, and axes for significance, using a permutation test of the F-statistic (999 permutations, $p < 0.05$) with the *anova. cca()* function of the 'vegan' package. To obtain a parsimonious RDA model, we applied forward selections of the explanatory variables with the *ordiR2step()* function ('vegan' package), and the application of the selection criterion of the best model by the adjusted R^2 of the model. This selection criterion reduces the risk of incorporating more variables than necessary into the model (Borcard et al., 2018). From partial RDAs (pRDAs) we quantified the variance explained by a set of environmental variables while controlling and adjusting the regression model by the effect induced by co-variables. The co-variables tested were: spatial (latitude, longitude), geomorphology, depth, hydrology variables (current and chlorophyll) together and separately.

On each island slope (Mayotte and Bassas da India), we quantified the overall spatial structure of the faunal dataset, which we decomposed into large, medium, and fine spatial scale sub-models, using distance-based Moran eigenvector map (dbMEM) analyses ('adespatial' package, *dbmem()* function). First, we applied RDAs between the response variables (taxon densities) after removing the trend from the dataset, and the explanatory spatial variables (called MEM for Moran Eigenvectors Map). Then, we used a permutation test of the RDA model to determine the significant axes and MEMs. The set of significant MEMs, which represent different scales of spatial structure, were then grouped together according to the spatial scales they represent. We applied new RDAs separately on the community dataset according to each set of explanatory spatial variables (large, medium, and fine scales) and we assessed significance of the axes. We examined the correlation between significant axes, representing large, medium, and fine scale patterns, and the environmental (explanatory) variables using multiple regressions for each significant spatial axis with the environmental factors (*lm()* function). We assessed the conditions of application – normality and variance homogeneity of the residuals – to validate the regression models.

Finally, we performed variation partitioning analyses of the faunal dataset (Hellinger-transformed density) by integrating different matrices of explanatory environmental variables (geomorphology, substrate, terrain, hydrology, large, medium, and fine scale spatial models) to quantify the percentages of variance explained by each set of environmental variables or each spatial structure, and their interrelationships ('vegan' package, *varpart()* function). We tested the fractions of variance explained by each matrix *via* a permutation test (*anova.cca()* function, $n = 999$ permutations, p-value <0.05) and represented these fractions using Venn diagrams.

3. Results

3.1. Seamounts and island slopes environmental characteristics

3.1.1. Hydrology (current, surface primary productivity, water mass)

Varying current (mean velocities from 0.004 to 0.4 m/s) have been modelled in the different bathymetric layers over the seamounts and island slopes (Table 2). In the deepest water layer (350–650 m), the Glorieuses terrace had the highest current speeds. Intermediate values were found in Sakalaves, Bassas da India, Hall, Jaguar, and the northern slope of Mayotte, while the lowest ones were estimated on the western and eastern slopes of Mayotte. In addition to strong surface and intermediate depth currents (from 0 to 200 m) (Supplem. mat. 6), the Sakalaves platform also had the highest surface current variability (Table 2). The current variability in the deepest layers was stronger on the seamounts, with a maximum on Glorieuses (0.19 m/s) than along the slopes of Mayotte and Bassas da India Islands (minimum 0.03 m/s). The daily averaged Chla concentration was the highest and the most variable on the eastern slope of Mayotte (0.20 ± 0.07 mg/m^3). Chla concentration was lower, comparable, and slightly variable on the other sites, although more variable on the island slopes. The concentration was globally higher in winter than in summer in the channel (by a factor of ~1.5), except in Bassas da India, where the average concentration varied poorly among seasons (Table 2, Supplem. mat. 6). The recorded hydrological parameters of the bottom waters (temperature, oxygen) differed among sites (Table 2, Supplem. mat. 6). The shallowest site of Sakalaves was crossed by warm and poorly oxygenated waters, characteristic of the Subtropical Surface Water mass (STSW), at the interface with the South Indian Central Water mass (SICW). The intermediate sites of Hall summit, Jaguar, and Bassas da India (453–623 m) were traversed by waters of intermediate temperatures and were highly oxygenated, characteristic of the SICW. The deeper areas (>700 m) explored on Hall Bank, the Glorieuses terrace and, for the most part of the western slope of Mayotte, were located in the colder, lower oxygenated Intermediate Antarctic Water mass (AAIW). Finally, the northern and eastern slopes of Mayotte explored along a broad bathymetric gradient, were traversed by the SICW, then AAIW and the Red Sea Intermediate Water mass (RSIW), characterized by low oxygen

Table 2
Summary of chlorophyll *a* concentrations, current velocities, temperature and oxygen, substrate diversity and hardness (mean ± standard deviation), BPI, slope, and depth gradient. For Chla and current velocities only those used for statistical analyses after removing collinear ones are shown.

Site	Winter Chla (mg/m^3)	Inter-annual Chla (mg/m^3)	Velocity 350–650 m (m/s)	std velocity 0–50 m (m/s)	std velocity 350–650 m (m/s)	Temperature (°C)	Oxygen (µmol/kg)	Substrate diversity	Hardness (1–6)	BPI 500 (m)	Slope (°)	Depth gradient (m)
Mayotte, West slope	0.163 ± 0.005	0.007 ± 0.001	0.007 ± 0.007	0.330 ± 0.008	0.081 ± 0.053	8.8 ± 1.1	182.0 ± 32.0	0.19 ± 0.37	1.53 ± 1.09	0.4 ± 5.2	7.1 ± 4.4	233.7
Mayotte, North slope	0.162 ± 0.004	0.007 ± 0.001	0.029 ± 0.014	0.373 ± 0.003	0.078 ± 0.071	10.9 ± 1.1	206.5 ± 32.1	0.36 ± 0.41	1.96 ± 1.32	−3.6 ± 12	10.5 ± 7.9	734
Mayotte, East slope	0.242 ± 0.083	0.020 ± 0.013	0.004 ± 0.008	0.276 ± 0.052	0.033 ± 0.042	9.1 ± 1.9	182.5 ± 43.5	0.25 ± 0.34	4.60 ± 1.97	8.5 ± 27.8	11.9 ± 8.7	625.6
Glorieuses	0.171 ± 0.001	0.009 ± 0	0.140 ± 0.001	0.333 ± 0	0.189 ± 0	7.4 ± 0.3	147.8 ± 12.9	0 ± 0	6.00 ± 0	0.1 ± 22.3	8.9 ± 10.9	158.7
Sakalaves	0.155 ± 0.001	0.008 ± 0	0.037 ± 0.007	0.607 ± 0.005	0.152 ± 0.012	14.3 ± 0.6	_	0.21 ± 0.33	5.21 ± 1.67	−3.7 ± 14.2	3.2 ± 3.1	113.4
Bassas da India	0.166 ± 0.001	0.029 ± 0	0.027 ± 0.003	0.417 ± 0.012	0.043 ± 0.064	11.1 ± 0.5	243.3 ± 5.0	0.27 ± 0.36	4.01 ± 1.77	5.3 ± 10.1	7.3 ± 6.1	169.1
Hall, summit	0.158 ± 0	0.015 ± 0.001	0.020 ± 0.003	0.495 ± 0.003	0.174 ± 0.003	11.0 ± 0.2	243.1 ± 0.7	0.17 ± 0.29	4.47 ± 1.18	0.2 ± 3.5	1.9 ± 2.3	84
Hall summit-slope	0.159 ± 0.001	0.014 ± 0.002	0.017 ± 0.002	0.492 ± 0.004	0.171 ± 0.003	10.1 ± 0.3	220.3 ± 29.0	0.32 ± 0.38	4.94 ± 1.19	−2.7 ± 19.8	10.6 ± 10.9	422.7
Jaguar	0.168 ± 0	0.008 ± 0	0.032 ± 0.001	0.473 ± 0	0.144 ± 0	11.2 ± 0.2	233.1 ± 2.3	0.37 ± 0.38	4.34 ± 1.92	2.5 ± 5.5	4.5 ± 2.8	93.1

concentrations and temperatures. The end of the western slope of Mayotte also intersects the RSIW layer boundary.

3.1.2. Geomorphology and topography

The composition and proportions of each geomorphological facies varied among sites. Their characteristics (depth-derived topographic indexes) are summarized in Table 2 and Supplem. mat. 6. The Glorieuses platform is a homogeneous and flat carbonate slab. The explored upper slope only slightly impacted the BPI 500 m which was minimum at this site. The eastern slope of Mayotte (12° average) has four types of geomorphological classes: soft sediment, carbonate geomorphology, mixed facies (volcanic relief, carbonate, and sedimentary substrates) and volcanic facies. A volcanic cone was present at the bottom of the slope (maximum BPI 500 m of 135.2 m high). The northern slope of Mayotte (10.5° average) is formed by a terrace, ending by a channel. Most of the slope substrate was composed of sediments, interrupted by an area of boulder-forming carbonate reliefs and long walls. The bottom of the slope was composed of volcanic landforms. The explored terrace on the western slope of Mayotte has a 7.1°-average slope and depth gradient less pronounced than the northern terrace. This dominant sedimentary geomorphology (78%) was interspersed with rocky reliefs resulting in high and variable small-scale BPI 60 m (~13 m difference in altitude). The Sakalaves platform is interspersed with faults and escarpments (Courgeon et al., 2016). The summit is composed of a carbonate slab (43%), a volcanic dyke zone interspersed with sedimentary substratum (mixed geomorphology), and an area of sediment dunes and ripples (Miramontes et al., 2019a). A 22°-escarpment was overhung by an area of volcanic landforms. On Bassas da India, the explored terrace along a low bathymetric gradient with a 7.3°-middle slope, showed a high BPI at 500 m. The upper slope is dominated by sediments, forming long sand dunes and ripples (Miramontes et al., 2019a), while the remaining part is predominantly composed of volcanic geomorphology forming irregular landforms (64.9%). Hall is a flat-topped bank whose summit has a rather flat, volcanic geomorphology (90.0%). Hall's Dive 12 crossed a terrace area which consisted predominantly of volcanic (60.9%) and mixed geomorphologies resulting in a high BPI 500 m. Finally, Jaguar has a flat-topped morphology with scarp networks. The bathymetric gradient explored, and the average slope were low. Three main geomorphologies were explored on the summit area: a sedimentary zone, a volcanic geomorphology zone, composed of lava flows forming lobes (52%), and a carbonate slab.

3.1.3. Substrate

Sedimentary substratum was dominant on the western and northern slopes of Mayotte, while rock proportions dominated on the other sites. Soft sediment areas were however present on Bassas da India and Sakalaves (ripple zones) (Fig. 2). The proportions of carbonate rock were high on the eastern slope of Mayotte and Sakalaves and covered the whole Glorieuses terrace. Volcanic substrate proportions were higher at sites south of the channel (Hall, Jaguar and Bassas da India) and consisted of mixed volcanic substrate with small sedimentary zones often in depression, or purely volcanic substrate. The eastern slope of Mayotte and Sakalaves also consisted of mixed bedrock (carbonate, volcanic), also present in Bassas da India and Hall, to a lesser extent. Gravel proportions on the northern and eastern slopes of Mayotte were higher than at the other sites. Biogenic substrate was observed mainly on the northern slope of Mayotte and consisted of coral skeletal and shell debris. Substrate diversity was higher on Jaguar, Mayotte's northern slope and Hall's dive 12 (summit-slope) than on the other sites (Table 2). The highest hardness indices were found on Glorieuses and Sakalaves and the lowest on the western and northern slopes of Mayotte. Comparative environmental conditions of sites mapped along dive transects are available in Supplem. mat. 7.

3.2. Structure of megabenthic assemblages

3.2.1. Inter-site variability

The highest taxa density was observed on the Glorieuses platform (779.8 ± 751.3 ind/200 m^2), which significantly differs from all the other sites, despite high intra-site variability (Table 3; graph available in

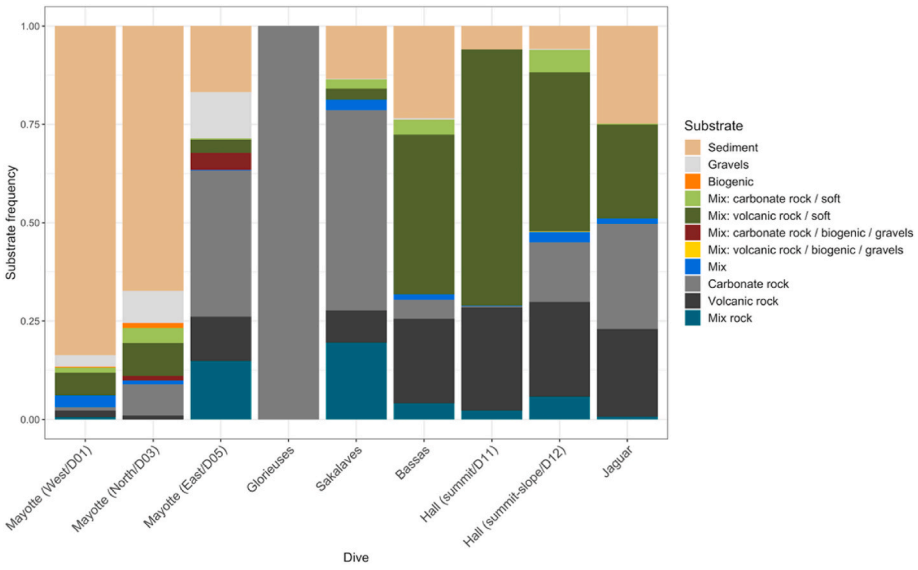

Fig. 2. Relative frequencies of substrate categories (analysed from all images by semi-automatic method) for each transect. (format: 1.5-column image).

Supplem. mat. 8). The eastern slope of Mayotte Island had intermediate densities (183.4 ± 169.3 ind/200 m^2), higher (> factor of 2) than those observed on the northern and western slopes, and significantly different from all the other sites except the Sakalaves and Jaguar mounds. Sakalaves platform had densities significantly higher than those observed on Hall Bank and Bassas da India island slopes where low densities occurred without significant difference with the northern and western slopes of Mayotte. Among these densities, the proportion of sessile fauna were the highest over Glorieuses and Jaguar while the lowest at Sakalaves (Table 3).

For the minimum sampling effort (n = 58 polygons), the eastern and northern slopes of Mayotte had the highest taxonomic richness (TR = 54 and 52, respectively) and higher than the western slope of the island (TR = 44). The sites in the center and south of the channel showed intermediate and comparable richness (37 < TR < 40), while the Glorieuses platform in the north had the lowest one (TR = 29) (Table 3; Supplem. mat. 9). With a greater sampling effort, taxonomic richness on the eastern slope of Mayotte would be higher than on the northern slope (from extrapolated richness at n = 400 polygons, TR = 83 and 73, respectively) (Table 3; Supplem. mat. 9). However, this extrapolation did not show a significant change in the richness of each site relative to the others.

We identified 99 taxa from the 8430 analysed images. Even compared at various taxonomic ranks including high ones (order, class), the composition showed a high variability among the studied seamounts and island slopes (Fig. 3). Most of the sites had a high relative frequency of habitat-forming taxa, but with different dominances among poriferan and cnidarian classes among sites. Indeed, the Glorieuses terrace was dominated by Demospongiae, the northern and western slopes of Mayotte by Anthozoa and Hexactinellida, Hall Bank by Anthozoa, Demospongiae and Hexactinellida, Bassas da India island slopes by Hexactinellida and Jaguar by Hydrozoa, i.e., Stylasteridae (incertae) and Demospongiae (Fig. 3). Cnidarian orders also showed distinct compositions and frequencies among sites, even among slopes of the same island. For example, the northern slope of Mayotte was dominated by Zoantharia (mainly non epiphytic Zoanthidae, and some epiphytic zoantharians), while the eastern slope by Hydrozoa (i.e., Stylasteridae (incertae)) and colonial scleractinian (i.e., *Enallopsammia*). Sakalaves and the summit of Hall Bank were dominated by solitary scleractinians, and Bassas da India by Antipatharia (Supplem. mat. 10). Brachiopods had high relative frequencies on Glorieuses and the eastern slope of Mayotte compared to the other sites. The eastern slope of Mayotte and the Sakalaves platform displayed a high relative frequency of mobile taxa, Gastropoda and Actinopterygii respectively, and a higher proportion of ophiuroids. Globally, fish had a higher relative frequency in the central/southern sites of the channel than in the northern ones. Details of the densities of each taxon per dive are available in Supplem. mat. 11. For the four taxa identified to lower taxonomic ranks (asteroids, echinoids, fish, and crustaceans) we also observed differences in composition and richness among the surveyed sites (Supplem. mat. 12).

Table 3
Summary of community metrics: mean taxa density/polygon (200 m^2) and standard deviation, proportion of sessile fauna (habitat-forming taxa, i.e., sponges and colonial cnidarians, solitary cnidarians, and brachiopods) to the total mean density, interpolated taxonomic richness for n = 58 polygons (TR 58) and estimated (Hill, q = 0) for n = 400 polygons (ES 400), and total beta diversity (BD) values for the nine transects.

Site	Mean density/ 200 m^2	% Sessile fauna	TR 58	ES 400	BD
Mayotte, West slope	89.4 ± 240.8	76.4	44	61	0.81
Mayotte, North slope	80.3 ± 131.0	67.2	52	73	0.79
Mayotte, East slope	183.4 ± 169.3	46.1	54	83	0.62
Glorieuses	779.8 ± 751.3	89.2	29	35	0.28
Sakalaves	148.3 ± 128.7	22.6	39	54	0.61
Bassas da India	31.5 ± 24.4	60	32	49	0.70
Hall, summit	70.9 ± 170.5	49.8	37	49	0.63
Hall, summit-slope	81.0 ± 93.4	72.8	39	60	0.69
Jaguar	139.9 ± 128.2	83.6	40	50	0.65

3.2.2. *Intra-site beta diversity*

The total beta diversity (BD) for all sites was high (from 0.61 to 0.81 out of 1), except for Glorieuses (BD = 0.28) (Table 3). The highest BDs were observed for the western and northern slopes of Mayotte, while it was lower over the eastern slope of Mayotte. The replacement (turnover) process of beta diversity was dominant at almost all sites (from 53% to 65%) compared with the abundance difference, except for Glorieuses and Jaguar where both processes contributed equally. The species contribution to beta diversity (SCBD) values ranged from 1.6% to 19.1%. In all sites, poriferans and cnidarians that are potentially habitat-forming taxa, had a high cumulative SCBD value, ranging from 18.7% on Glorieuses to 45.5% on Hall's dive 12 (summit-slope) (Fig. 4A). These

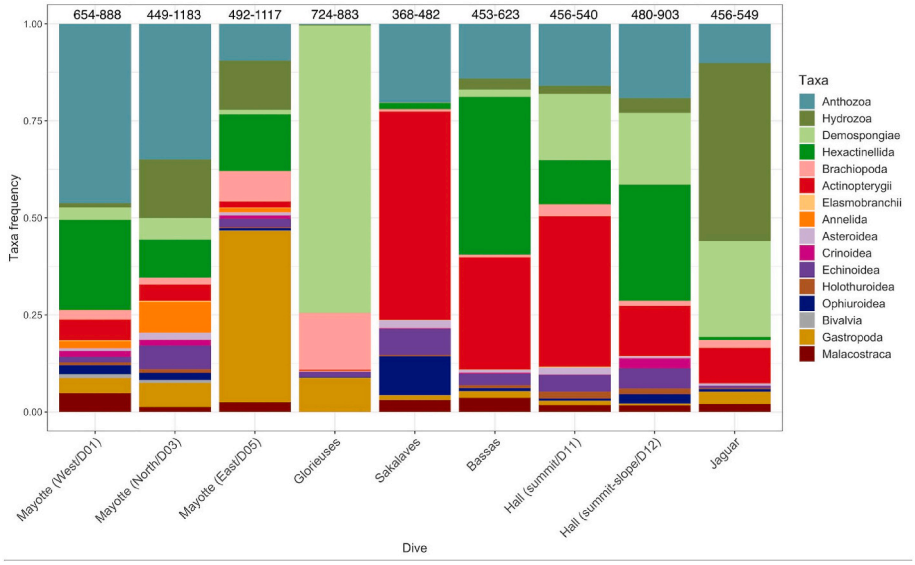

Fig. 3. Relative frequencies of megabenthic taxa whose identification was aggregated to phylum or class rank for each transect. Depth range (in m) of each transect is specified at the top of each bar. The first five taxa represented (upper colour classes) are sessile (Anthozoa to Brachiopoda), the other taxa represented are mobile. (format: 2-column image).

taxa comprised notably Hexactinellida, Demospongiae, Stylasteridae, Antipatharia, solitary scleractinians, Alcyonacea, Pennatulacea, Actiniaria and the scleractinian *Enallopsammia*. Brachiopoda contributed to the variability along most of the sites as well but to a lower extent (2–6%). Mobile taxa contributed also to the total BD, with a cumulative contribution ranging from 28.3% on the summit-slope of Hall up to 56.3% observed on Sakalaves. The urchin *Stereocidaris* displayed the greatest contribution on the northern slope of Mayotte (12.4%) and on Glorieuses (9.6%). *Micropyga* urchins had high contributions, particularly *Micropyga* sp2 (9%) on Glorieuses and *Micropyga* sp1 (6.9%) on Sakalaves. Crustaceans also contributed to the variability along the transects, such as *Glyphocrangon* (8.13%) on the western slope of Mayotte or *Puerulus carinatus* (5.30%) on Sakalaves. A fish of the genus *Chlorophthalmus* was generally observed as the first contributing taxon on Sakalaves, Bassas da India, Hall and Jaguar (5.9%–15.9%). Finally, the Gastropoda group was among the first contributing taxa on the slopes of Mayotte and Glorieuses (6–8%). Depending on the seamount and island slope, some geomorphological facies concentrated a great number of polygons with significant LCBDs (Local Contribution to Beta Diversity), such as sedimentary facies on the northern and western slopes of Mayotte, volcanic facies on Sakalaves, Hall summit and Bassas da India, or mixed facies on a slope on Hall dive 12 (summit-slope) (Fig. 4B). At some sites, polygons with significant LCBDs were scarce and located at transitions between substrates such as Jaguar Bank (sediment-carbonate, volcanic-sediment) or between different topographies (summit/upper slope) like on the Glorieuses carbonate platform (between −11.389° latitude and 47.275° longitude).

3.2.3. Multiscale assemblage variability

From the biogeographic network analysis applied on the whole dataset, we delineated 45 groups, half of which correspond to multispecific clusters indicating faunal assemblages generated by a limited number of highly abundant taxa. The remaining groups correspond to monospecific patches each composed of a single taxon, either locally highly abundant or with a very low density (rare taxon observed in at most 5 polygons). Out of the 45 total groups, 12 assemblages were the most represented in the area since they were present in at least 30 and at most 363 polygons, out of a total of 1608 over the nine camera transects. These 12 assemblages are multispecific clusters (except for the monospecific patch A9, ophiuroids) and are dominated by a few highly abundant taxa. Despite their low indicator value for their assigned assemblage, these taxa had high fidelity values - they were present in almost all polygons belonging to the cluster -, indicating that this criterion drove the cluster delineation. These “ubiquitous” taxa were generally those identified at higher taxonomic ranks. The main indicator taxa of each of the 12 assemblages (illustrated in Fig. 5) had indicator values (IndVal) between 20 and 75%, except for Hexactinellida (15.8%), but according to the biogeographical network, it was the indicator taxon for A3, because of its fidelity within this assemblage (99.6%), i.e., it was found in practically all the polygons in it (description of fidelity, specificity and indicator value in Supplem. mat. 13).

The 12 assemblages displayed patchy distributions within each site or transect (Fig. 6) ranging from large (2 km, e.g., on the Glorieuses or upper slope of Bassas da India) to small patch size (0.06 km, e.g., on the northern slope of Mayotte, Hall summit-slope), thus representing different scales of assemblage variability. Assemblage dominance and spatial pattern differed also among sites (seamounts, island slopes) and among the three slopes of Mayotte Island. For example, the A1 assemblage (Demospongiae, Brachiopoda, *Micropyga* sp2 sea urchins) formed the largest patch on Glorieuses. The A2 (characterized by vagile taxa with the *Chlorophthalmus* and Pleuronectiformes fish, the *Puerulus carinatus* shrimps, some echinoids, and asteroids) occurred at sites of the center and south of the channel where it formed very large aggregations. The A4 (Gastropoda and Paguroidea) formed large patches only over the Glorieuses and the eastern slope of Mayotte, while the A5 (Stylasteridae incertae) was dominant over Jaguar and formed larger patches than over the eastern slope of Mayotte and the other sites. Other assemblages formed smaller patches like A14 (*Stereocidaris* sea urchins and Bivalvia) over the northern slope of Mayotte Island, but larger patches than over Bassas da India island slope. A8 (Alcyonacea, Comatulida) also had a very scattered distribution, for example over the eastern slope of Mayotte Island, Bassas da India island slope or Hall (summit-slope). We also observed differences in composition between the northern sites (Mayotte, Glorieuses) and the southern ones, for a few assemblages (e.g., A2, A4, A6).

3.3. Environmental drivers of megabenthic assemblage patterns

3.3.1. Environmental drivers of inter-site differences in community metrics

Current velocity at 350–650 m showed a significantly positive relationship with faunal density ($p = 0.002$, adjusted $R^2 = 0.82$), but negative with taxonomic richness as well as with total beta diversity (p

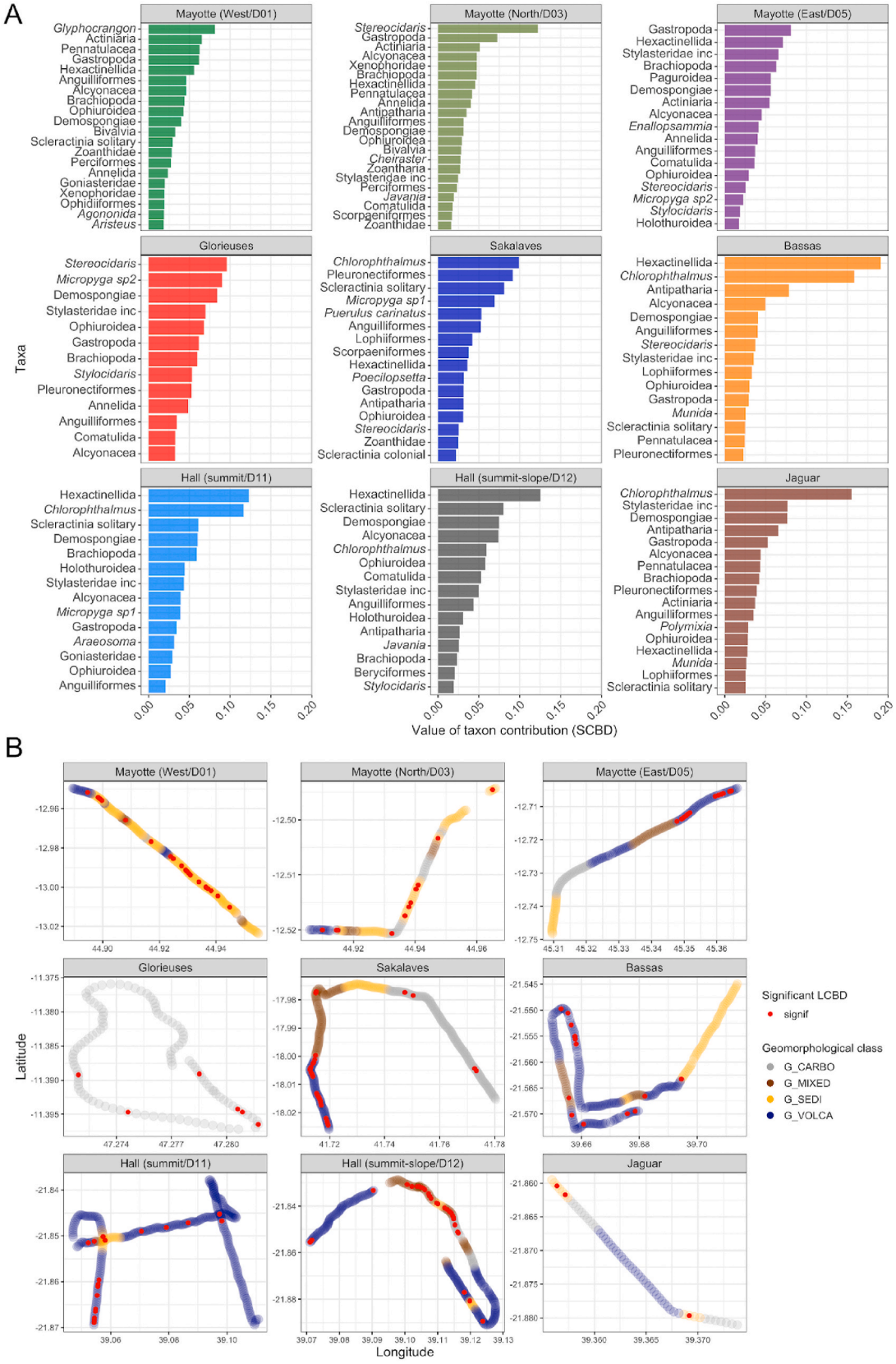

Fig. 4. **(A)** Histograms representing taxa with SCBD (Species Contribution to Beta Diversity) values higher than the transect mean, for each transect. **(B)** Maps representing analysis polygons along the camera tow tracks at each dive site with significant LCBD (Local Contribution to Beta Diversity) values (999 permutations, $p < 0.05$) (red dot), i.e., with a unique taxa composition, for each transect, superimposed with the geomorphological classes. (format: 2- column image).

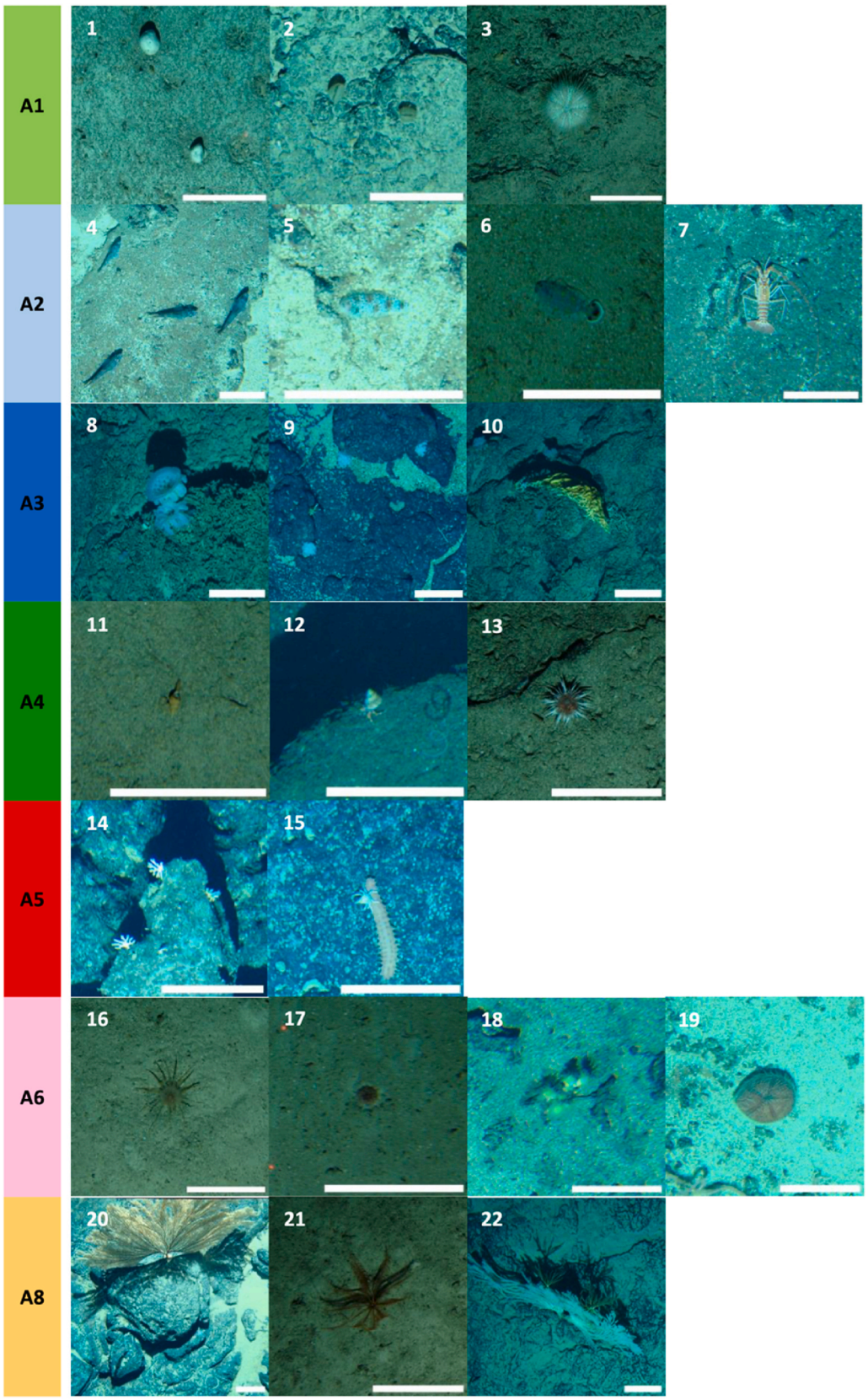

Fig. 5. Illustrative images of the contributing taxa from the 12 assemblages observed along seamounts and island slopes. 1 – Demospongiae; 2 – Brachiopoda; 3 – *Micropyga* sp2; 4 – *Chlorophthalmus*; 5 – Pleuronectiformes; 6 – *Poecilopsetta*; 7 – *Puerulus carinatus*; 8 – *Aphrocallistes* sp.; 9 – Hexactinellida; 10 – *Enallopsammia*; 11– Gastropoda; 12 – Paguroidea; 13 – *Caenopedina* sp.; 14 – Stylasteridae incertae; 15 – Epialtidae over an Holothuroidea; 16, 17 – Scleractinia (solitary); 18 – Scleractinia (colonial); 19 – *Heterobrissus*; 20 – Alcyonacea; 21 – Comatulida; 22 – Comatulida over a large Alcyonacea coral; 23 – Ophiuroidea; 24, 25 – Antipatharia; 26 – Annelida; 27 – *Javania* sp.; 28 – *Micropyga* sp1; 29, 30 – Goniasteridae asteroids; 31, 32 – Actiniaria; 33 – Synodontidae; 34 – *Stereocidaris*; 35 – Bivalvia (Propeamussidae). The white bar represents a 20 cm unit. (format: 2-column image).

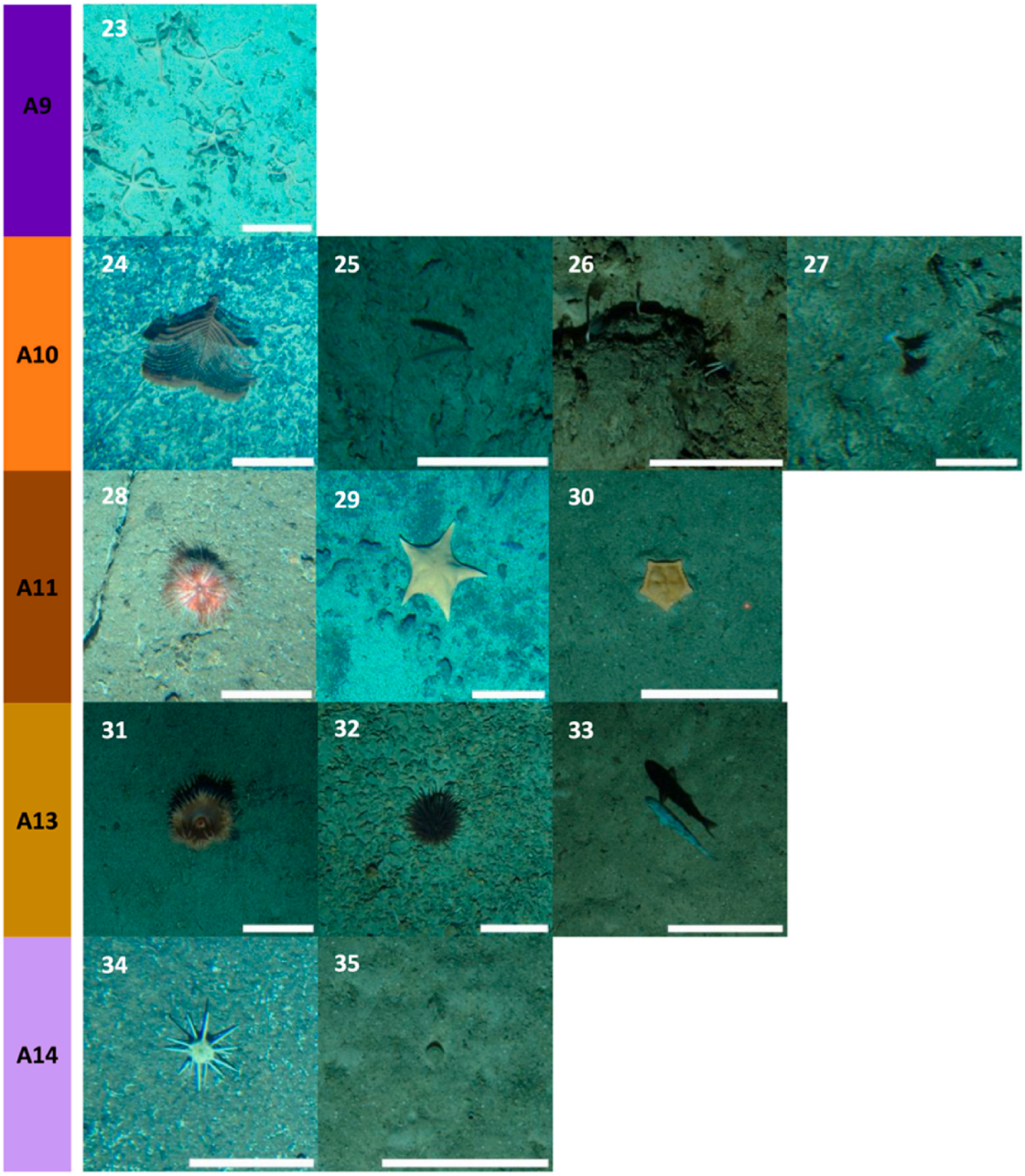

Fig. 5. (*continued*).

= 0.0015, adjusted $R^2 = 0.75$) (Supplem. mat. 14). Variability in current velocity at 350–650 m also showed a significantly negative relationship with taxonomic richness ($p = 0.0373$). Winter and mean minimum Chla also showed significant but weak positive relationships with richness. The percentage cover of carbonate geomorphology showed a significantly positive relationship with mean faunal density ($p = 0.0002$, adjusted $R^2 = 0.86$), as well as a significantly negative relationship with total beta diversity ($p = 0.0002$, adjusted $R^2 = 0.73$). On the contrary, the percentage coverage of sedimentary geomorphology showed a significantly positive relationship with total beta diversity ($p = 0.0394$, adjusted $R^2 = 0.40$). Distance to the Madagascar coast showed a significantly negative non-linear relationship with faunal density while positive for the distance to the Mozambique coast. Substrate hardness showed a significant but weak negative non-linear relationship with taxonomic richness ($p = 0.0478$), which shows an optimum for intermediate hardness between 4.5 and 5 out of a total of 6. A negative relationship between hardness and BD was significant. The substrate diversity showed a significant negative relationship with mean faunal density while positive with total beta diversity.

3.3.2. *Environmental drivers of the assemblage's composition at multiscale*

The partial redundancy analysis (pRDA) applied to the assemblages showed that 16.7% of the variance was explained by the significant environmental variables after forward selection of the model variables ($p < 0.05$, 999 permutations, $R^2 = 0.16$), and 7.9% by the spatial variables (latitude, longitude) (Fig. 7). Axes 1 to 9 were significant, implying that many axes explained relatively little variance. The A2 assemblage (*Chlorophthalmus*, Pleuronectiformes and other mobile fauna) and the A6 (solitary and colonial Scleractinia) mainly found at Sakalaves and Hall, were strongly positively correlated with high current variability between 0 and 50 m and current speed at 350–660 m (Fig. 7). These conditions also favored the A11 (*Micropyga* sp1) found mainly at the Sakalaves and Hall sites. These assemblages were positively correlated with carbonate or sedimentary geomorphologies with a

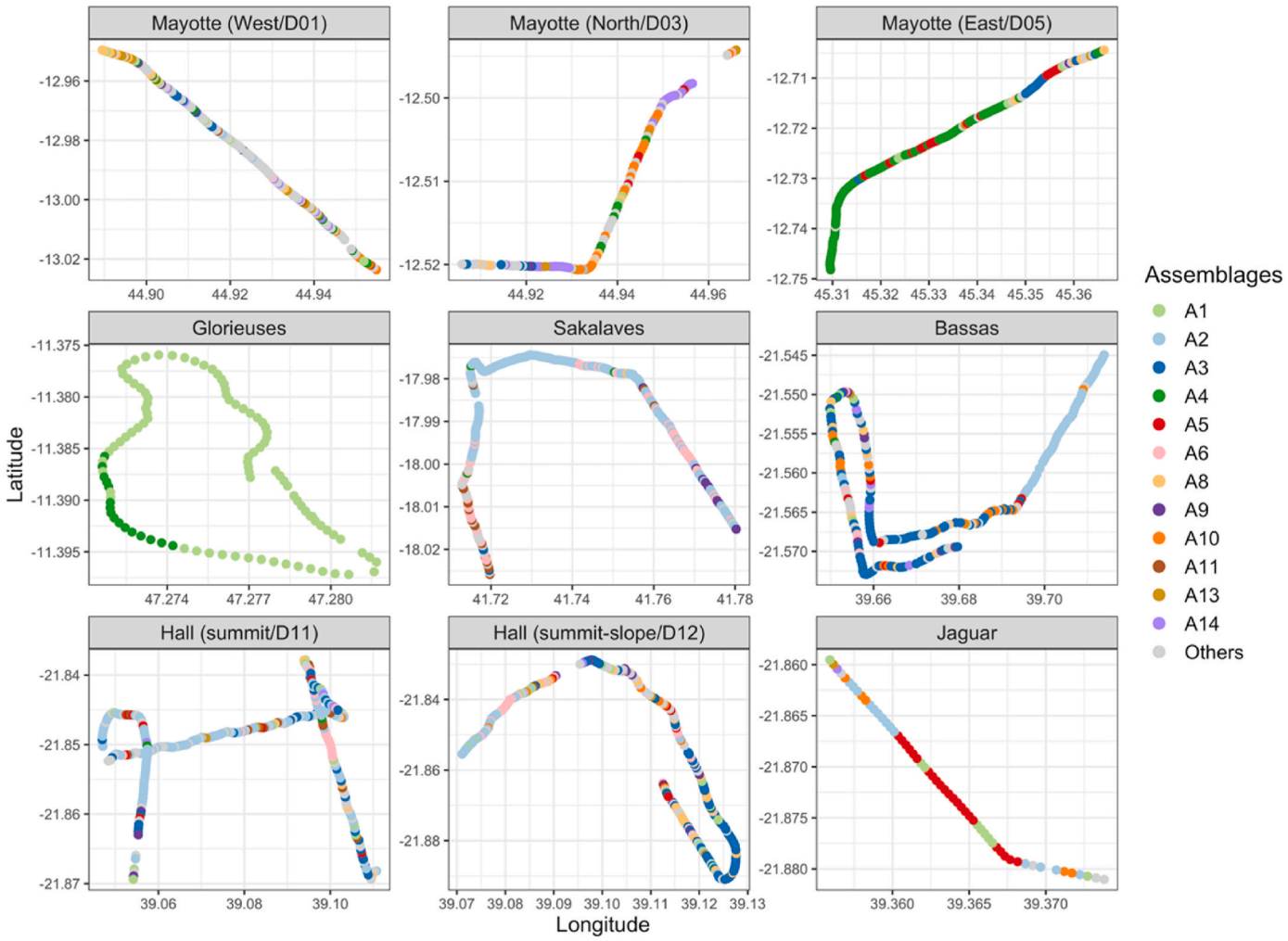

Fig. 6. Map of the 12 most represented assemblages (each assemblage is found in at least 30 polygons) within the Mozambique Channel, obtained from a biogeographic network analysis. (format: 2- column image).

few reliefs. The A3 (Hexactinellida including *Aphrocallistes*, the scleractinian *Enallopsammia* for the eastern slope of Mayotte) was mainly found at Bassas da India, Hall (dive12, summit-slope) and on the eastern slope of Mayotte and was strongly positively correlated with high values of depth and slope, as well as with BPI 500 m, high rugosity, volcanic rock and inter-annual Chla variability. The A8 (Alcyonacea, Comatulida) was strongly positively correlated with the presence of volcanic geomorphology, mainly on Bassas da India and Hall's dive 12 (summit-slope). The A13 (mainly Actiniaria) was positively correlated with intermediate substrate diversity values, in areas of volcanic geomorphology mainly composed of mixed volcanic/sediment substrate. The A5 (Stylasteridae) was positively correlated with substrate hardness and substrate diversity and was found mainly at sites on the eastern and northern slopes of Mayotte, as well as on Jaguar and Hall. The A14 (*Steredocidaris*), A18 (Pennatulacea) and A24 (*Glyphocrangon*) were poorly represented on this triplot but appeared to be slightly correlated with the presence of sedimentary geomorphology. Finally, the gravel, eastness and winter Chla variables contributed to the dispersion of sites on axis 2, correlated with the A1 (Demosponges, Brachiopoda, *Micropyga* sp2) and the A4 (Gasteropoda, Paguroidea), also driven by substrate hardness. Hydrology explained 15.3% of the variation in assemblage structure, 6.9% of which did not overlap with the other variables (Fig. 8A). We observed an equal pure contribution of topography and substrate (1.7% each). Topography and hydrology together explained 4.7% of the variation. In total, geomorphology explained 6.5% of the variation, with the major part (3.5%) overlapping with substrate. The fraction of variance purely explained by space was low (0.8%), however, we observed a high overlap of variance explained by hydrology and space (2.8%) (Fig. 8B).

3.3.3. Spatial structures and environmental drivers of beta-diversity along Mayotte and Bassas da India island slopes

The spatial analysis (dbMEM) detected spatial structures at large (~2–6 km), medium (~0.8–2 km) and small (~0.1–0.5 km) scales which were all significant along the western and eastern slopes of Mayotte Island and the Bassas da India's one (results of the dbMEM analysis in Supplem. mat. 15). Along the northern slope of Mayotte, only large- and medium-scale spatial structures were significant. The environmental variables explained 20.3% of the community structure variation, of which 7.6% were spatially structured at medium-scale, and 5.3% were at large scale (Fig. 9A). Along the eastern slope, the main part of the community variation was explained by a medium-scale spatial structure (20.5%) of which 16.1% represented medium-scale-structured environmental variables (Fig. 9B). Conversely to the other sites, a fine-scale spatial structure contributed to the community variation along the eastern slope of Mayotte (6.1%), half of which represented a significant pure spatial fraction that was not correlated with environmental variables. Along the western slope of Mayotte, the main part of the variance were residuals (92%). Along the Bassas da India slope, the environmental variables explained 25.8% of the community dataset variance, of

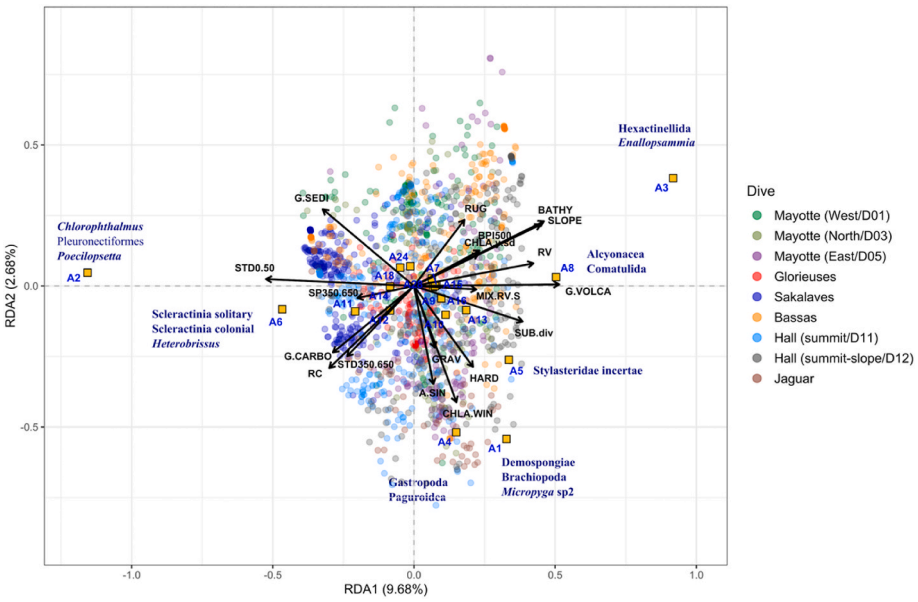

Fig. 7. Partial Redundancy Analysis (pRDA) (triplot, scaling 2) applied to the assemblage densities after quadratic and Hellinger transformation of the data. The conditional co-variables of the model are latitude and longitude. The significant variables of the model, obtained after a forward selection and test of the significant variables (n = 999 permutations), are shown. Refer to Supplem. mat. 13 and Fig. 5 for the description of the assemblages. Abbreviation of abiotic variables in the plot: SP350.650 = current velocity at 350–650 m depth, STD350.650 = current velocity variability at 350–650 m depth, CHLA. y.sd = interannual chlorophyll *a* concentration variability, CHLA. WIN = winter chlorophyll *a* concentration, G. SEDI = sedimentary geomorphology, G. VOLCA = volcanic geomorphology, G. CARBO = carbonate geomorphology, BATHY = bathymetry, RUG = rugosity, A. SIN = eastness orientation of slope, RV = volcanic rock, RC = carbonate rock, GRAV = gravels, MIX. RV.S = mixed volcanic rock/sediment, HARD = substrate hardness, SUB. div = substrate diversity. (format: 2-column image).

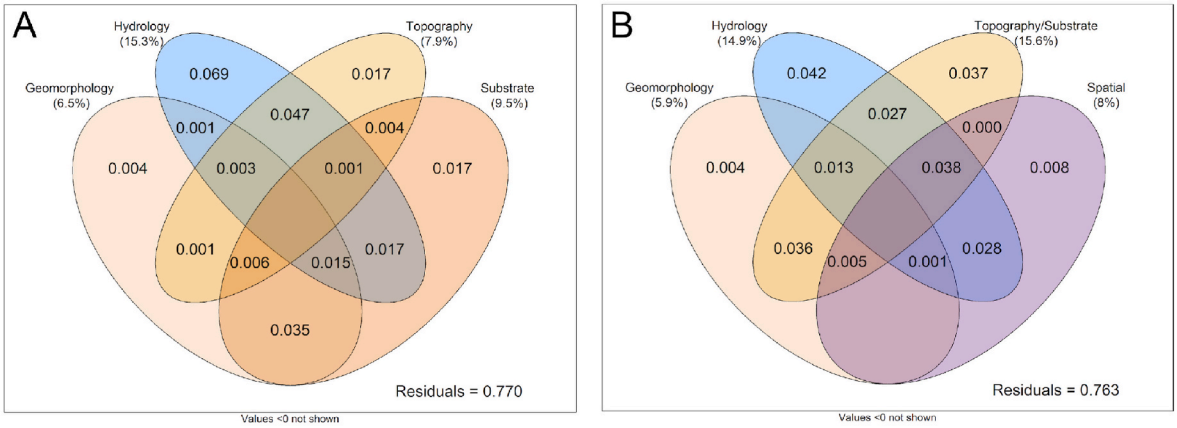

Fig. 8. Venn diagrams representing the contributions of the different sets of explanatory variables from a variation partitioning analysis of the assemblage dataset. **(A)** Without integration of spatial variables (latitude, longitude), **(B)** With integration of spatial variables. The numbers indicate the fractions of variation explained by each set of environmental variables. Negative contributions are not shown. (format: 2-column image).

which 16.3% represented broadly structured environmental variables (not shown). Parts of these spatial structures can be interpreted with the environmental variables considered in the study. The large-scale spatial structure along the northern slope of Mayotte (at ~3 km-scale) was significantly related to depth, slope, BPI 500 m, volcanic geomorphology, and substrate composition (gravels and biogenic bottoms). The medium-scale (~1 km) spatial structure was significantly related to BPIs, sedimentary geomorphology, and substrate diversity. Along the eastern slope of Mayotte, the medium-scale spatial structure (~0.8–1 km) was significantly related to the three types of geomorphological facies, BPIs, nature, hardness and diversity of the substratum, depth, as well as the value and the orientation of the slope (Supplem. mat. 15).

Partial redundancy analyses (pRDA) along each slope revealed in more detail the community structure with the environmental variables. Along the northern slope of Mayotte, high value of hard substrate was positively correlated with high abundances of mainly habitat-forming taxa together with other taxa (e.g., Comatulida) separated along the first axis from taxa associated with areas dominated by sediment (Fig. 10A). The polygons with significant LCBD were in sedimentary geomorphological zones (where volcanic rocks are sparsely distributed) as well as in volcanic zones. On the eastern slope of Mayotte, Hexactinellida (including the large-size *Aphrocallistes*), the scleractinian *Enallopsammia* and Comatulida were positively correlated with high values of slope, volcanic substrate, and bottom elevation variability (BPI 500 m) (Fig. 10B). Gastropoda and Demospongiae were inversely correlated with depth and slope. Finally, Brachiopoda and Stylasteridae were positively correlated with north and east slope orientation. Sites contributing to the BD (LCBD) were found in areas of volcanic geomorphology and associated with volcanic, carbonate, or mixed substrates, steep slopes, or high large-scale BPI. Very low variances were

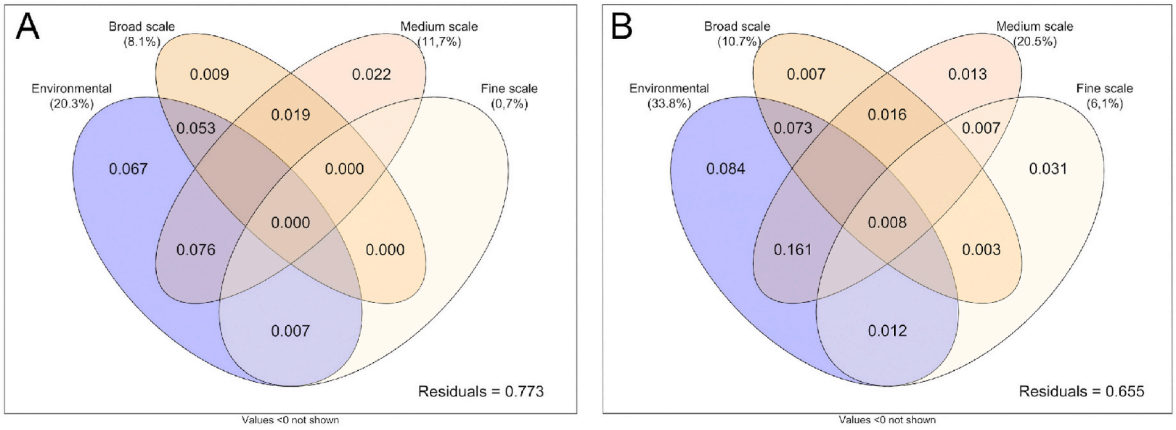

Fig. 9. Venn diagrams representing the contributions of the different sets of explanatory variables (environment, large, medium, and fine scale spatial structures) derived from a variation partitioning analysis of the community dataset. The large-, medium- and fine-scale spatial structures were obtained from an analysis of Moran eigenvector maps based on geographical distances (dbMEM). **(A)** Northern slope of Mayotte, **(B)** Eastern slope of Mayotte. (format: 2-column image).

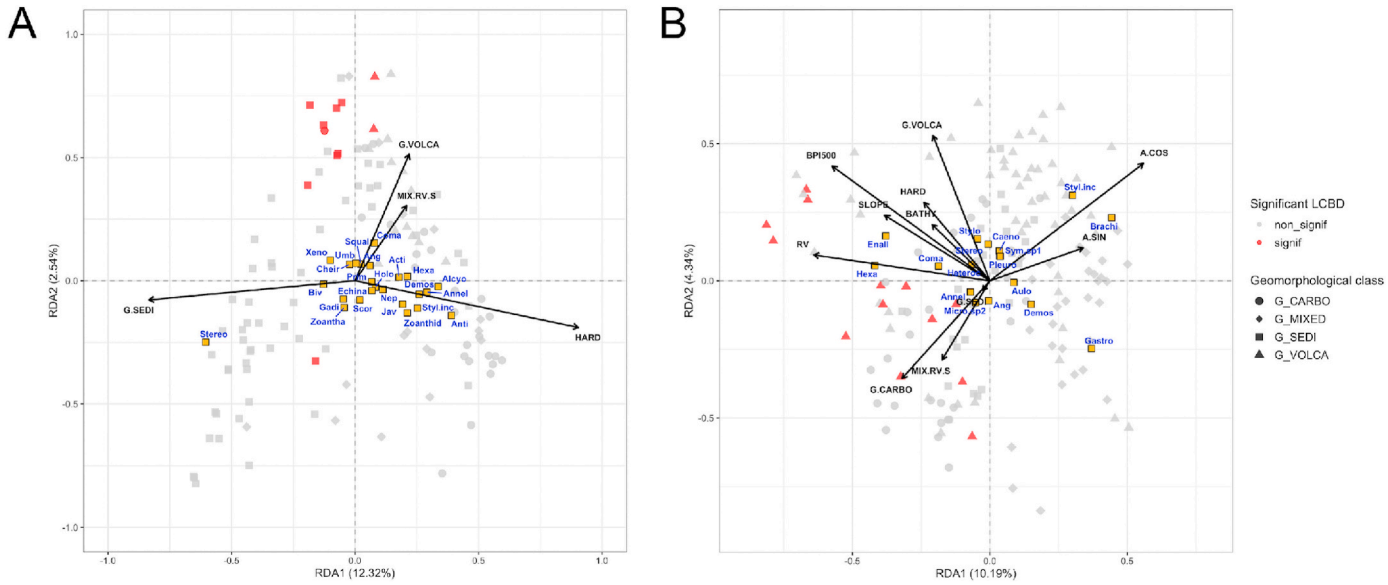

Fig. 10. Partial Redundancy Analysis (pRDA) (triplot, scaling 2) applied to taxon densities after quadratic and Hellinger transformation of the data. The conditional co-variables of the model are latitude and longitude. For each RDA, only the significant variables of the model are shown, obtained after a forward selection and testing of the significant variables (n = 999 permutations). **(A)** Northern slope of Mayotte, **(B)** Eastern slope of Mayotte. Red dots indicate unique sites with significant LCBD values. (format: 2-column image).

explained along the western slope of Mayotte, from the pRDA (not shown), with substrate hardness and depth as the two significant variables, differentiating soft-bottom from hard-bottom communities. Along the Bassas da India slope, a low variance (8.7 %) was explained by the abiotic variables, while 19.3% by the spatial variables (pRDA not shown). The fish *Chlorophthalmus* was positively correlated with sedimentary substrate on the upper terrace. Hexactinellida was positively correlated with high substrate hardness values and with low carbonate rock and curvature ones. Antipatharia and Alcyonacea were positively correlated with deep areas having high BPI 500 m (large elevation difference, sloping area). Sites contributing to the BD (LCBD) were found in areas of volcanic or mixed geomorphology associated with higher curvature. The maps of the significant large-, medium- and fine-scale spatial patterns along the island slopes are available in Supplem. mat. 16.

4. Discussion

4.1. Variability of community metrics and composition among seamounts and island slopes along the Mozambique channel

At the same latitude along the Mozambique Channel, seamounts displayed higher faunal densities than along island slopes (four-to ten-fold higher in the north and two to three-fold higher in the south). Higher biomass on seamount compared to continental slope were also reported in the southwest Pacific, mainly driven by the scleractinian *Solenosmilia variabilis* (Rowden et al., 2010b). In the Mozambique Channel, faunal densities were generally low, and the highest density observed on seamounts was mainly due to the high proportion of Demospongiae colonising flat carbonate morphologies over the Glorieuses seamount (~75% of its total density), and of Demospongiae and Stylasteridae on the Jaguar Bank. Nevertheless, the high density on Sakalaves platform was mainly driven by benthic fish. Variability of megafaunal community characteristics among seamounts has been

observed in some regions to be driven by currents (Genin et al., 1986; Kaufmann et al., 1989), surface productivity (Clark and Bowden, 2015; Bridges et al., 2022), depth gradient (Williams et al., 2011; Schlacher et al., 2014; Boschen et al., 2015; Clark and Bowden, 2015; Lapointe et al., 2020) and substrate (e.g., Sautya et al., 2011; Boschen et al., 2015; Morgan et al., 2015; Lapointe et al., 2020) but such relationships need to be confirmed in other oceanic regions, notably those with low productivity, such as in the Indian Ocean or central Pacific (Clark et al., 2012). In the present dataset, densities varied among seamounts by a factor of ten with a decreasing density from north to south (~1400 km) along the Mozambique Channel. Sautya et al. (2011) observed globally lower mean densities over seamounts in the northeast Indian Ocean, and differences up to about a factor four between seamounts distant from ~200 km. Similarly to seamounts, island slopes densities decreased with latitude along the Mozambique Channel, but also among slopes of the same island (Mayotte) of a factor two. Differences were explained by bottom current speed (between 350 and 650 m deep) and coverage of carbonate slab characterizing the flat top seamount morphologies found on the Glorieuses platform, and on parts of the Sakalaves' summit. The Northeast Mozambique Current (NEMC) in conjunction with the westerly flowing South Equatorial Current, strongly and permanently impacts the Glorieuses platform in the north of the channel (Collins et al., 2016). The presence of mesoscale eddies over this seamount and over the Davies Ridge to which the Sakalaves terrace belongs may provide favorable conditions for the establishment of high-density communities. Indeed, these eddies can integrate particulate material from the surface down to 1500 m deep (de Ruijter et al., 2002) by advection of the Mozambique and Madagascar terrestrial material offshore (Tew-Kai and Marsac, 2009). Benthic fauna density was also positively correlated with the distance of seamounts and island slopes to the Madagascar coast, from which surface water of higher productivity can be exported offshore, particularly with the NEMC. The high faunal densities found along the eastern slope of Mayotte, higher than those found along the two other slopes, can be explained by these inputs, but also by higher concentrations of Chla, despite weak modelled currents. The proximity of this slope to the lagoon and to the island (~2 km) would benefit from release of runoff of land materials and from the dense network of rivers (Faivre et al., 2020), in addition to input from the Madagascar coast from the NEMC.

Beta diversity also differed among the analysed sites. The quantification of substrates has enabled evidence of non-linear negative relationships between taxonomic richness and beta diversity with substrate hardness. A significant positive correlation of percentage sediment cover (hardness equivalence) with beta diversity was also reported in Shen et al. (2021). It is worth noting that in our study, beta diversity was also positively correlated with substrate diversity including various hard substrates such as carbonate and volcanic rocks. A more complex seabed would favor richer communities' settlement by providing additional habitat niches, as previously reported in Morgan et al. (2019) but without distinction between different hard substrates. This is exemplified along the western and northern slopes of the Mayotte Island, mainly composed of sedimentary areas interspersed by discontinuous rocky bottom (carbonate or volcanic), blocks and volcanic areas, adding complexity to the habitat.

Depth was not identified as a driver of diversity or density differences among the studied sites. However, depth is a proxy of many covariates, such as temperature and oxygen concentration that characterized water masses and energy flow in the system, linked to organisms' physiology (Thistle, 2003). While water masses were not tested in our study, these factors would potentially influence differences in richness and beta diversity among the explored features according to the water masses they encompass (Henry et al., 2015; Victorero et al., 2018; Auscavitch et al., 2020a). For example, Mayotte island slopes encompass three different water masses (SCIW, AAIW, RSW) over a larger bathymetric gradient which can promote higher richness and beta-diversity than the Glorieuses platform which resides mainly inside the AAIW. Nevertheless, the absence of a significant role of depth and latitude over the whole dataset could reflect the relatively restricted depth gradient explored for most sites, and an insufficient level of taxonomic identification to establish a relationship with the richness component.

Taxonomic composition varied among the studied seamounts and island slopes, even for taxa identified at a high taxonomic rank including habitat-forming taxa (anthozoan Orders, sponge Classes) or mobile ones. Sessile fauna usually dominated the assemblages, but some seamounts dominated by soft bottoms (Sakalaves terrace) were dominated by mobile fauna (fish and ophiuroids). Similarly, echinoderms dominated the summit of one of the Andaman Seamounts (north-eastern Indian Ocean) covered with fine sediment, while flanks and other sites with hard bottoms were dominated by sponges (Sautya et al., 2011). Such a discrepancy between dominance of suspension feeders (e.g., cnidarians and/or sponges) and mobile fauna (echinoderms, holothurians, predators) was reported between seamounts or guyots within the same regions, including the Mediterranean (Bo et al., 2020), off southern and central California (Lundsten et al., 2009) and off Chile where differences occur between oceanic islands and close seamounts dominated by mobile fauna and predators, and remote seamounts dominated by sessile/hemisessile suspension and deposit feeders (Tapia-Guerra et al., 2021). Many of the habitat-forming taxa identified in our study were common to several seamounts and island slopes, because of the low identification ranks achieved but we observed substantial frequency differences, meaning that the different sites are characterized by different biogenic habitats (e.g., Demospongiae at Glorieuses, cnidarians and Hexactinellida along the Mayotte island slopes, various proportion of Anthozoa and Hydrozoa among the three slopes). Identification efforts at lower ranks for four taxonomic groups (echinoids, asteroids, decapods, and fishes) enabled us to observe ubiquitous taxa over the channel such as echinoids and galatheids genera (e.g., *Stereocidaris*, *Stylocidaris*, *Munida*) while other groups seemed to be restricted to a few sites (*Glyphocrangon* decapods on Mayotte slopes, sea urchins *Heterobrissus* on Sakalaves, and *Pourtalesia* on the Glorieuses, *Chlorophthalmus* fish in the center and south of the channel). However, our dataset did not allow us to discuss biogeographic patterns at larger scale of these taxa due to the lack of biological data (e.g., genetic connectivity, dispersal capacity), spatial coverage over seamounts (mainly limited to summit relying on one-two camera transects) and the coarse taxonomic resolution. Comparison of our observations with other faunal datasets sampled in the channel and on the Mozambique/Madagascar margins would allow further exploration of this question. While the regional scale of our study focused on a comparison at the seamount level by considering each seamount as an own ecosystem, it is not excluded that seamounts on the southern part *vs.* northern part of the Mozambique channel act as a whole ecosystem on themselves respectively, regarding e.g., their water masses boundaries, organic matter fluxes, species interactions and connectivity (Watling and Auster, 2021).

4.2. Environmental drivers of the assemblage spatial patterns at multiscale

The biogeographic network analysis separated 12 main faunal assemblages dominated by a few highly abundant taxa with indicator values above 20%. The high faunal contribution to assemblages by a small number of abundant taxa, mentioned by Goode et al. (2021) and observed in other previous studies on seamounts (e.g., Boschen et al., 2015; Morgan et al., 2019), reflects the high spatial variability of megabenthic communities. The analysis has revealed assemblages displaying a highly patchy distribution, at varying spatial scales within seamounts and island slopes ranging from 0.06 km (e.g., along the western and northern slope of Mayotte) to ~2.5 km (e.g., the Glorieuses). This as well as differences among sites distant from 4 km to 1400 km along the Mozambique Channel. Patchy distribution of megabenthic communities is a pattern commonly observed on seamounts (Schlacher et al., 2014; Boschen et al., 2015; Clark and Bowden, 2015; Du Preez

et al., 2016; de la Torriente et al., 2018; Morgan et al., 2019; Shen et al., 2021) and is likely related to high habitat heterogeneity.

Hydrology, including both currents at different depths and surface primary production, was identified as one of the structuring factors, highlighting the complex and highly turbulent hydrographic regime that characterizes the Mozambique Channel (Hancke et al., 2014). The strong influence of the current at the Sakalaves and in less extent to Hall seamounts probably reflects the role of the intense eddies extending over the water column and exporting particulate material from the Mozambique coast down into the core of the eddies (Marsac et al., 2014), which could further enrich at least the Sakalaves seamount (close to the Mozambique coast). *Chlorophthalmus* fish feed on small pelagic crustaceans (e.g., mysids, euphausiids, copepods) (Anastasopoulou and Kapiris, 2008), and could indirectly benefit from such enhanced productivity. Ophiuroids were as well densely packed on the same site and would also benefit from enhanced productivity derived from eddies activity providing small particles such as fecal matter to feed on (Stöhr et al., 2012). While not analysed in the paper, flow direction could also have an influence on the source of larval supply (Lima et al., 2020).

Geomorphology, together with topography and substrata have a relatively strong contribution (24%) as structuring factors of megabenthic spatial patterns. Interestingly, different assemblages and habitat-forming taxa were associated with two types of rocky bottoms: the volcanic geomorphologies were colonized by hexactinellids and large cnidaria (e.g., alcyonaceans, scleractinian *Enallopsammia*), whereas on the carbonate slab areas we observed massive demosponges and brachiopods as well as solitary scleractinians. It is likely that differences in the (micro)topography characterizing these two geomorphologies (e.g., complexity of reliefs, rugosity) play a role in the preferential rocky habitats of these taxa (Giusti et al., 2014; Du Preez et al., 2016; Bargain et al., 2017; Standaert et al., 2023). Indeed, volcanic areas were often correlated with other abiotic conditions highlighted in our data (higher roughness, sloping areas, high BPI). The characterization effort of rocky substratum types is useful as it revealed differences in associated megabenthic communities. Furthermore, assemblages dominated by Alcyonacea and Hexactininellida were associated with slopes. Several previous studies have highlighted the presence of dense communities of cnidarians and sponges preferentially located in steep or sloping areas over seamounts (Hall-Spencer et al., 2007; Du Preez et al., 2016; de la Torriente et al., 2018; Bridges et al., 2021) but had not pointed out differences among Porifera classes. It was suggested that the interaction of currents over sloping areas generates increased flow and particulates mixing creating favorable habitats for these suspension feeders (Genin et al., 1986). Besides, our data showed that hydrology and topography had a shared contribution (~5%) underlining these potential interactions between currents and seamounts topographies affecting the communities. Moreover, seabed orientation (i.e., eastness, northness) reflects the seafloor exposure to water movement (Wilson et al., 2007). The high demosponge densities on Glorieuses and Jaguar terraces were strongly positively associated with eastness, even on relatively flat bottoms, which suggests the influence of currents from the Madagascar coast on the Glorieuses terrace, and of currents affecting the Sakalaves terrace from North to South that interact along escarpments (Miramontes et al., 2019a). Finally, except on sedimentary areas found on summits over large areas affected by currents (sedimentary ripples or dunes) or along island slope terraces and gravel areas colonized by specific faunal assemblages, hard-bottom communities dominate the seamounts and island slopes studied in the Mozambique Channel.

Along the Mayotte eastern slope, where the depth gradient is the largest, the lower temperature and oxygen content of the AAIW water mass at depth (compared to SICW at a shallower depth) may partially explain the sharp change in community composition, with the presence of quite dense habitats of large size hexactinellid *Aphrocallistes* and colonial scleractinian *Enallopsammia*. Our results showed these groups were favored by other factors (steep slope, high BPI revealing volcanic cone elevation as well as volcanic substrate), which have a greater contribution in explaining the variance of community structure than depth itself along this slope. The presence of a prominent volcanic cone in the deep part of this slope, where we observed these habitat-forming taxa, could also locally generate accelerated and turbulent flow (internal waves, mesoscale eddies) influencing larval dispersion (Stashchuk and Vlasenko, 2021) and/or favoring nutrient mixing and trapping of sinking POC (Morgan et al., 2019).

4.3. Spatial structures within seamounts and island slopes (beta diversity)

High beta diversities have been previously reported within seamounts and were generally related to a large depth gradient and to water mass hydrological variation (e.g., BDtot = 0.92 over 2400 m (Victorero et al., 2018); BDtot = 0.83 over 1200 m (Shen et al., 2021)). Except for the Glorieuses terrace, we also observed a high beta diversity within the different seamounts and island slopes (BDtot from 0.61 to 0.81), despite the low explored depth gradients at the different sites (90–730 m), and the coarse level of identification of some taxa. These high beta diversity values have been explained by the high habitat heterogeneity related to substrate and topography, as well as the geomorphologies of the seamounts over the horizontal gradient (7-km to16-km transects). It was not surprising to observe low levels of beta diversity on Glorieuses, due to the strong but stable current conditions and the presence of a carbonate slab alone, thus providing fewer niches and transition zones. Morgan et al. (2019) have also reported high beta diversities within a narrow depth range that could be attributed to the large horizontal gradient explored providing high habitat differences within the same depth layer. Furthermore, the replacement component of beta diversity was prevalent in the abundance difference of taxa, as reported along seamount slopes (Victorero et al., 2018; Morgan et al., 2019; Goode et al., 2021). Despite the oligotrophy of the Mozambique Channel, the highly turbulent water regime (i.e., upwellings and mesoscale eddies) may contribute to the nutrient supply (Lévy et al., 2001) and contribute to sustain taxa turnover as in productive areas (Brault et al., 2013; Victorero et al., 2018).

On each site, many of the taxa detected as strong contributors to total beta diversity were sessile cnidarians and sponges that potentially form habitats for other taxa. Although their identification rank was poorly resolved, these taxa generate variability within seamounts and island slopes through their patchy distribution, characterized by high local abundances. At finer identification ranks, we would expect even higher levels of beta diversity along each transect, for these taxa and their associates (de la Torriente et al., 2020). As observed at regional scale among seamounts, mobile taxa, including particular genera of fish, decapods, or sea urchins, also contributed to the BD within individual seamount or island slope. Their distributions were localized in specific locations (with significant contributions to beta diversity i.e., with unique compositions of faunal assemblages) that we identified as abrupt changes of substrate or topography (interface areas). Volcanic areas gather many of these specific locations, highlighting their role in creating habitat and enhancing faunal heterogeneity. The high number of specific locations on the sedimentary facies along the two other slopes of Mayotte Island was explained by the heterogeneity of these areas dominated by soft sediment but scattered by numerous rocky blocks and boulders. Change in substratum influenced the distribution of sessile fauna according to their attachment mode, as well as of some mobile taxa such as *Glyphocrangon* shrimps observed exclusively over sedimentary bottom types along the western slope of Mayotte, or cidaroid sea urchins mainly observed over hard-bottom types where their chance to prey sponges and corals is enhanced (Lawrence and Jangoux, 2020). However, cidaroids have flexible feeding mode and their distributional pattern appears to be constrained by food availability more than substrate type (Lawrence and Jangoux, 2020). For instance, *Stereocidaris* sea urchins were observed on soft sediments on the northern slope of Mayotte, where they can feed on seabed material or foraminifera

(Lawrence and Jangoux, 2020). Recruitment processes may also influence the spatial distribution pattern of some taxa, such as *Stereocidaris*, *Stylocidaris* and *Micropyga* sea urchins, for which larval recruitment may occur in the same place depending on the current regime and the nature of the substrate, which could explain proximity among specimens (personal communication, Dr. Thomas Saucède). Influence of the social behavior of *Chlorophthalmus* fish (indicator of A2) observed forming schools on the images would explain the large patches they form. The gregarious behavior of *Puerulus carinatus* decapods (Fischer and Bianchi, 1984) may explain the high local abundances of this species over Sakalaves rocky bottoms, where it counts among the top five contributors to beta diversity.

Significant spatial structures in the community composition were identified along the outer slopes of Mayotte and Bassas da India, with differences among slopes in the dominant scale of variation. Medium scale (~1 km) structures were dominant along the northern and especially the eastern slopes of Mayotte Island, while the broad scale (~2 km) was dominant for the Bassas da India slope. Bassas da India's external slope is indeed characterized by the dichotomy of two geomorphologies, an almost flat upper terrace with sand waves and a rough volcanic area deeper along the slope, whose curvature and sloping areas support completely distinct communities. Along the northern slope of Mayotte Island, contrasts between sedimentary areas and areas with hard substrate contributed the most to the variance of the community. The eastern slope of Mayotte communities showed the highest complex spatial patterns, with medium- (~20%), large- (~11%) and fine-scale (~6%) structures, suggesting several scales of environmental heterogeneity. The medium-scale (~1 km) pattern was explained by the high environmental heterogeneity along this slope (superimposition of the role of depth gradient to slope/topography and the geomorphology/substrate heterogeneity). This heterogeneity is notably due to volcanic structures, usually larger than the sparse blocks found on the two other slopes of Mayotte Island spread over seabed types dominated by sediment. We could not explain small scale spatial structures with the environmental factors, although observed by e.g., the assemblage's variability (Fig. 6). The resolution of our polygons (i.e., sampling units of 60-m linear) was probably not sufficient to capture the environmental heterogeneity at these spatial scales. For example, high vertical blocks sparsely distributed over flat sedimentary bottom along the Mayotte western slope were not revealed at the resolution of the DTM bathymetric model, but were colonized by a strikingly different fauna compared to the surroundings. This was however likely reflected in the hardness variable that appeared as a main driver of megabenthic communities along this slope. The fraction of the variation not explained by the environmental variables, corresponding to the spatial structure alone, and which was significant at fine scale along the eastern slope of Mayotte, may reflect unmeasured processes such as the potential presence of stochastic and population dynamic (e.g., species association, especially with small-size fauna not identified from images, competition, and predation). It can also reflect potential environmental drivers that we did not consider in this analysis, but which play a role in the community structure at this scale (Peres-Neto and Legendre, 2010).

The scale of the spatial structures identified depends on our smallest sampling unit and the level of taxonomic identification achieved as well. Population dynamics would probably be better characterized from fine resolution taxonomic rank. However, the low faunal densities of the study area have required gathering data into larger sampling units and may explain the difficulty to relate small spatial patterns. Nevertheless, even considering high identification rank, we were able to highlight a strong patchy community structure over different spatial scales, especially for habitat-forming taxa, which responded to various scales of environmental drivers. Sponges and cnidarians are key components of seamount or other deep-sea ecosystem functioning (Beazley et al., 2013; Buhl-Mortensen et al., 2016; de la Torriente et al., 2020). Further insight on their spatial structure at finer resolution and structuring role may be interesting using a functional angle view. To overcome the difficulties of identifying these taxa on images, a morpho-functional approach would allow a more detailed analysis of cnidarian and sponge communities (Hanafi-Portier et al., unpublished results). These suspension feeders can be indicators of flow and turbidity levels (Schönberg, 2021) as they adapted their morphologies to environmental conditions. Such sponge morphological proxies could compensate for difficulties to obtain reliable hydrological measures at small spatial scales, relevant to explain faunal distribution patterns.

5. Conclusion

This study shows that megabenthic community structure on seamounts and along island volcanic slopes in the Mozambique Channel is structured at various spatial scales in response to imbricated scales of environmental heterogeneity, particularly noticeable in the channel complex geological history context. This is a critical point to consider in future studies to describe and understand community and benthic habitat structuration in the region. Particularly, the main results revealed:

- High density differences among seamounts (by a factor of 10), and among Mayotte island outer slopes (by a factor of 2). Higher densities over seamounts compared to island slopes at the same latitude, explained by strong currents and flat geomorphology. Megabenthic assemblage structures differ also among seamounts with significant differences in dominant taxa even identified at high taxonomic ranks (Porifera classes or Cnidaria orders).
- A north-south difference in composition for a few faunal assemblages whose indicator taxa were identified at the genus level (e.g., galatheids, echinoids and fishes), suggesting potential biogeographic patterns along the channel. However, additional sampling effort and higher taxonomic resolution are needed to further explore this contribution to regional scale differences.
- Despite a low taxonomic resolution, high levels of beta diversity (~0.60–0.80) on seamounts and island slopes, except on the flat carbonate terrace of the Glorieuses archipelago (0.28). Differences among sites were explained by substrate diversity. Both habitat-forming and mobile taxa contribute to the beta-diversity whose spatial scales (0.06–2 km) are highly variable among sites especially on volcanic substrates or associated with changes in geomorphologies.
- Various environmental drivers play a role in shaping megabenthic assemblages over different spatial scales. Hydrology (current, primary productivity) was an important driver, along with interaction with geomorphology (> km), topography (60–500 m) and substrate (60 m). The rocky nature (volcanic *vs.* carbonate) and associated microtopography explained substantial differences in benthic communities. This highlights the importance to consider rock bottom type specificities in future studies.
- Within island slopes, km-scale megabenthic community structures were explained by seabed topography and substrate, but the smaller-scale assemblage variability was hardly explained by the environment due to the low faunal densities and the high level of diversity in our study area. Also, increasing the resolution of bathymetric and hydrodynamic models, and monitoring currents at relevant scales would be helpful to understand current/topography/substrate interactions and their impact on benthic communities.
- It is worth noting that Mayotte island slopes and Glorieuses terrace, strongly differ in their benthic community densities, taxonomic richness, composition, and beta diversity as well as scales of spatial patterns. These differences and the scales of habitat heterogeneity are important elements to consider for the management of the Mayotte and Glorieuses deep-sea ecosystems, which are integral parts of marine protected areas.

Author contributions

Mélissa H–P: Conceptualization, Data curation, Formal analysis, Investigation, Methodology, Visualization, Writing/original draft, Writing/review & editing. **Sarah Samadi:** Conceptualization, Funding acquisition, Investigation, Methodology, Project administration, Supervision, Writing/review & editing. **Laure Corbari:** Conceptualization, Funding acquisition, Investigation, Methodology, Resources, Supervision, Writing/review & editing. **Marion Boulard:** Data curation, Writing/review & editing. **Elda Miramontes:** Data curation, Writing/review & editing. **Pierrick Penven:** Formal analysis, Resources, Writing/review & editing**. Boris Leroy:** Resources, Software, Writing/review & editing. **Thibault Napoléon:** Resources, Software. **Stéphan J. Jorry:** Writing/review & editing. **Karine Olu:** Conceptualization**,** Formal analysis, Funding acquisition, Investigation, Methodology, Project administration, Supervision, Writing - original draft, Writing/review & editing.

Funding

The BioMaGlo cruise and project were supported by funding from the Xth European Development Fund (Fonds Européen de Développement; FED) "sustainable management of the natural heritage of Mayotte and the Eparses Islands" program managed by the French Southern and Antarctic Lands (Terres Australes et Antarctiques Françaises; TAAF) with the support of the Mayotte Departmental Council (Conseil Départemental de Mayotte), the French Development Agency (Agence Française de Développement; AFD) and the European Union. The PAMELA project (PAssive Margin Exploration LAboratories) is a scientific project managed by IFREMER and TotalEnergies in collaboration with Université de Bretagne Occidentale, Université Rennes 1, Université Pierre et Marie Curie, CNRS and IFPEN. The thesis of Mélissa Hanafi-Portier is co-funded by TotalEnergies and IFREMER as part of the PAMELA (Passive Margin Exploration Laboratories) scientific project.

Declaration of competing interest

The authors declare the following financial interests/personal relationships which may be considered as potential competing interests:

HANAFI-PORTIER reports financial support was provided by TotalEnergies SE. OLU reports financial support was provided by TotalEnergies SE. SAMADI reports financial support was provided by TotalEnergies SE. SAMADI reports financial support was provided by the Xth European Development Fund (Fonds Européen de Développement; FED). HANAFI-PORTIER reports a relationship with TotalEnergies SE that includes: funding grants.

Data availability

Data will be made available on request.

Acknowledgements

The authors would like to thank the captains, officers, and crews of RV's *L'Antea*, *L'Atalante*, *Le Pourquoi Pas?* and the SCAMPI towed-camera team for their contribution and assistance with data acquisition. We also would like to thank the chief scientists and scientific team of the BIOMAGLO (https://doi.org/10.17600/17004000), PTOLEMEE (https://doi.org/10.17600/14000900), BATHYMAY (Pol Guennoc; https://doi.org/10.17600/4200020), PAMELA-MOZ01, and PAMELA MOZ04 (Gwénaël Jouet and Éric Deville) cruises and the PAMELA project leaders (Jean-François Bourillet, Philippe Bourges, and Jean-Noël Ferry) (https://doi.org/10.18142/236). We are grateful to the engineer implied in the project: Julie Tourolle for assisting in the analysis of GIS data, Catherine Borremans and Olivier Soubigou for assisting with the image annotations and GIS development requirement, Marie Eve-Julie Pernet for the processing of the fauna samples used to help faunal identification from images, Christophe Brandily for helping in the curation and treatment of the CTD data, and Charline Guerin for the reprocessing of the DTM resolution (bathymetric data). We also would like to thank Simon Courgeon for helping in the geomorphological units' interpretation, Louise Keszler for the primary annotation of the images of BIOMAGLO, and the students of ISEN for the substrate algorithm development. We are also grateful to Tim W. Nattkemper and Daniel Langenkämper for allowing the image data loading and their annotation using Biigle 2.0 and for their technical support. We are grateful to all the taxonomists who have contributed to the identification of the fauna in the images and in the collections: Nicolas Puillandre (gastropods); Philippe Maestrati (bivalves); Éric Pante and Daniela Pica (cnidarians); Paco Cardenas and Cécile Debitus (poriferans); Enrique Macpherson (galatheids); Tin-Yam Chan (crustaceans); Wei-Jen Chen, Jhen-Nien Chen, Mao-Ying Lee and Paul Giannasi (fishes); Thomas Saucède (echinoids) and Christopher Mah (asteroids). We are grateful to the two reviewers for their time and constructive reviews, which helped to improve the manuscript.

Appendix A. Supplementary data

Supplementary data to this article can be found online at https://doi.org/10.1016/j.dsr.2023.104198.

References

Althaus, F., Williams, A., Schlacher, T., Kloser, R., Green, M., Barker, B., Bax, N., Brodie, P., Hoenlinger-Schlacher, M., 2009. Impacts of bottom trawling on deep-coral ecosystems of seamounts are long-lasting. Mar. Ecol. Prog. Ser. 397, 279–294. https://doi.org/10.3354/meps08248.

Anastasopoulou, A., Kapiris, K., 2008. Feeding ecology of the shortnose greeneye Chlorophthalmus agassizi bonaparte, 1840 (pisces: chlorophthalmidae) in the eastern ionian sea (eastern mediterranean). J. Appl. Ichthyol. 24, 170–179. https://doi.org/10.1111/j.1439-0426.2007.01028.x.

Audru, J.-C., Guennoc, P., Thinon, I., Abellard, O., 2006. Bathymay : la structure sous-marine de Mayotte révélée par l'imagerie multifaisceaux. Compt. Rendus Geosci. 338, 1240–1249. https://doi.org/10.1016/j.crte.2006.07.010.

Auscavitch, S.R., Deere, M.C., Keller, A.G., Rotjan, R.D., Shank, T.M., Cordes, E.E., 2020a. Oceanographic drivers of deep-sea coral species distribution and community assembly on seamounts, islands, atolls, and reefs within the Phoenix islands protected area. Front. Mar. Sci. 7, 42. https://doi.org/10.3389/fmars.2020.00042.

Auscavitch, S.R., Lunden, J.J., Barkman, A., Quattrini, A.M., Demopoulos, A.W.J., Cordes, E.E., 2020b. Distribution of deep-water scleractinian and stylasterid corals across abiotic environmental gradients on three seamounts in the Anegada Passage. PeerJ, b 8, e9523. https://doi.org/10.7717/peerj.9523.

Baco, A.R., Morgan, N.B., Roark, E.B., 2020. Observations of vulnerable marine ecosystems and significant adverse impacts on high seas seamounts of the northwestern Hawaiian Ridge and Emperor Seamount Chain. Mar. Pol. 115, 103834 https://doi.org/10.1016/j.marpol.2020.103834.

Bargain, A., Marchese, F., Savini, A., Taviani, M., Fabri, M.-C., 2017. Santa maria di Leuca province (mediterranean sea): identification of suitable mounds for cold-water coral settlement using geomorphometric proxies and maxent methods. Front. Mar. Sci. 4 https://doi.org/10.3389/fmars.2017.00338.

Beazley, L.I., Kenchington, E.L., Murillo, F.J., Sacau, M. del M., 2013. Deep-sea sponge grounds enhance diversity and abundance of epibenthic megafauna in the Northwest Atlantic. ICES (Int. Counc. Explor. Sea) J. Mar. Sci. 70, 1471–1490. https://doi.org/10.1093/icesjms/fst124.

Bo, M., Coppari, M., Betti, F., Massa, F., Gay, G., Cattaneo-Vietti, R., Bavestrello, G., 2020. Unveiling the deep biodiversity of the janua seamount (ligurian sea): first mediterranean sighting of the rare atlantic bamboo coral chelidonisis aurantiaca studer, 1890. Deep Sea Res. Oceanogr. Res. Pap. 156, 103186 https://doi.org/10.1016/j.dsr.2019.103186.

Borcard, D., Gillet, F., Legendre, P., 2018. Numerical Ecology with R, Use R! Springer International Publishing, Cham. https://doi.org/10.1007/978-3-319-71404-2.

Boschen, R., Rowden, A., Clark, M., Barton, S., Pallentin, A., Gardner, J., 2015. Megabenthic assemblage structure on three New Zealand seamounts: implications for seafloor massive sulfide mining. Mar. Ecol. Prog. Ser. 523, 1–14. https://doi.org/10.3354/meps11239.

Bourillet, J.-F., Ferry, J.-N., Bourges, P., 2013. PAMELA : Passive Margins Exploration Laboratories. https://doi.org/10.18142/236.

Braga-Henriques, A., Porteiro, F.M., Ribeiro, P.A., de Matos, V., Sampaio, I., Ocaña, O., Santos, R.S., 2013. Diversity, distribution and spatial structure of the cold-water coral fauna of the Azores (NE Atlantic). Biogeosciences 10, 4009–4036. https://doi.org/10.5194/bg-10-4009-2013.

Brault, S., Stuart, C.T., Wagstaff, M.C., McClain, C.R., Allen, J.A., Rex, M.A., 2013. Contrasting patterns of α- and β-diversity in deep-sea bivalves of the eastern and

western North Atlantic. Deep Sea Res. Part II Top. Stud. Oceanogr. 92, 157–164. https://doi.org/10.1016/j.dsr2.2013.01.018.
Bridges, A.E.H., Barnes, D.K.A., Bell, J.B., Ross, R.E., Howell, K.L., 2022. Depth and latitudinal gradients of diversity in seamount benthic communities. Journal of Biogeography jbi 14355. https://doi.org/10.1111/jbi.14355.
Bridges, A.E.H., Barnes, D.K.A., Bell, J.B., Ross, R.E., Howell, K.L., 2021. Benthic assemblage composition of south atlantic seamounts. Front. Mar. Sci. 8, 660648 https://doi.org/10.3389/fmars.2021.660648.
Buhl-Mortensen, L., Vanreusel, A., Gooday, A.J., Levin, L.A., Priede, I.G., Buhl-Mortensen, P., Gheerardyn, H., King, N.J., Raes, M., 2010. Biological structures as a source of habitat heterogeneity and biodiversity on the deep ocean margins: biological structures and biodiversity. Mar. Ecol. 31, 21–50. https://doi.org/10.1111/j.1439-0485.2010.00359.x.
Buhl-Mortensen, P., Buhl-Mortensen, L., Purser, A., 2016. Trophic ecology and habitat provision in cold-water coral ecosystems. In: Rossi, S., Bramanti, L., Gori, A., Orejas, C. (Eds.), Marine Animal Forests. Springer International Publishing, Cham, pp. 1–26. https://doi.org/10.1007/978-3-319-17001-5_20-1.
Castelin, M., Delavenne, J., Brisset, J., Chambart, C., Corbari, L., Keszler, L., Lozouet, P., Olu, K., Poncet, L., Puillandre, N., Samadi, S., 2017. Exploration et étude de la biodiversité benthique profonde de Mayotte et des îles éparses (Rapport final de la convention MNHN-TAAF dans le cadre du Xème FED régional «gestion durable du patrimoine naturel de Mayotte et des îles Eparses).
Charles, C., Pelleter, E., Révillon, S., Nonnotte, P., Jorry, S.J., Kluska, J.-M., 2020. Intermediate and deep ocean current circulation in the Mozambique Channel: new insights from ferromanganese crust Nd isotopes. Mar. Geol. 430, 106356 https://doi.org/10.1016/j.margeo.2020.106356.
Cho, W., Shank, T.M., 2010. Incongruent patterns of genetic connectivity among four ophiuroid species with differing coral host specificity on North Atlantic seamounts. Mar. Ecol. 31, 121–143. https://doi.org/10.1111/j.1439-0485.2010.00395.x.
Clark, M.R., Bowden, D.A., 2015. Seamount biodiversity: high variability both within and between seamounts in the Ross Sea region of Antarctica. Hydrobiologia 761, 161–180. https://doi.org/10.1007/s10750-015-2327-9.
Clark, M.R., Rowden, A.A., Schlacher, T., Williams, A., Consalvey, M., Stocks, K.I., Rogers, A.D., O'Hara, T.D., White, M., Shank, T.M., Hall-Spencer, J.M., 2010. The ecology of seamounts: structure, function, and human impacts. Ann. Rev. Mar. Sci 2, 253–278. https://doi.org/10.1146/annurev-marine-120308-081109.
Clark, M.R., Schlacher, T.A., Rowden, A.A., Stocks, K.I., Consalvey, M., 2012. Science priorities for seamounts: research links to conservation and management. PLoS One 7, e29232. https://doi.org/10.1371/journal.pone.0029232.
Collins, C., Hermes, J.C., Roman, R.E., Reason, C.J.C., 2016. First dedicated hydrographic survey of the Comoros Basin. J. Geophys. Res.: Oceans 121, 1291–1305. https://doi.org/10.1002/2015JC011418.
Corbari, L., Samadi, S., Olu, K., 2017. BIOMAGLO Cruise, RV Antea. https://doi.org/10.17600/17004000.
Courgeon, S., Bachèlery, P., Jouet, G., Jorry, S.J., Bou, E., BouDagher-Fadel, M.K., Révillon, S., Camoin, G., Poli, E., 2018. The offshore east African rift system: new insights from the Sakalaves seamounts (Davie Ridge, SW Indian Ocean). Terra. Nova 30, 380–388. https://doi.org/10.1111/ter.12353.
Courgeon, S., Jorry, S.J., Camoin, G.F., BouDagher-Fadel, M.K., Jouet, G., Révillon, S., Bachèlery, P., Pelleter, E., Borgomano, J., Poli, E., Droxler, A.W., 2016. Growth and demise of Cenozoic isolated carbonate platforms: new insights from the Mozambique Channel seamounts (SW Indian Ocean). Mar. Geol. 380, 90–105. https://doi.org/10.1016/j.margeo.2016.07.006.
Courgeon, S., Jorry, S.J., Jouet, G., Camoin, G., BouDagher-Fadel, M.K., Bachèlery, P., Caline, B., Boichard, R., Révillon, S., Thomas, Y., Thereau, E., Guérin, C., 2017. Impact of tectonic and volcanism on the Neogene evolution of isolated carbonate platforms (SW Indian Ocean). Sediment. Geol. 355, 114–131. https://doi.org/10.1016/j.sedgeo.2017.04.008.
Davies, J.S., Stewart, H.A., Narayanaswamy, B.E., Jacobs, C., Spicer, J., Golding, N., Howell, K.L., 2015. Benthic assemblages of the anton dohrn seamount (NE atlantic): defining deep-sea biotopes to support habitat mapping and management efforts with a focus on vulnerable marine ecosystems. PLoS One 10, e0124815. https://doi.org/10.1371/journal.pone.0124815.
de la Torriente, A., Aguilar, R., González-Irusta, J.M., Blanco, M., Serrano, A., 2020. Habitat forming species explain taxonomic and functional diversities in a Mediterranean seamount. Ecol. Indicat. 118, 106747 https://doi.org/10.1016/j.ecolind.2020.106747.
de la Torriente, A., Serrano, A., Fernández-Salas, L.M., García, M., Aguilar, R., 2018. Identifying epibenthic habitats on the Seco de los Olivos Seamount: species assemblages and environmental characteristics. Deep Sea Res. Oceanogr. Res. Pap. 135, 9–22. https://doi.org/10.1016/j.dsr.2018.03.015.
de Ruijter, W.P.M., Aken, H.M. van, Beier, E.J., Lutjeharms, J.R.E., Matano, R.P., Schouten, M.W., 2004. Eddies and dipoles around South Madagascar: formation, pathways and large-scale impact. Deep Sea Res. Oceanogr. Res. Pap. 51, 383–400. https://doi.org/10.1016/j.dsr.2003.10.011.
de Ruijter, W.P.M., Ridderinkhof, H., Lutjeharms, J.R.E., Schouten, M.W., Veth, C., 2002. Observations of the flow in the Mozambique channel. Geophys. Res. Lett. 29, 140–141. https://doi.org/10.1029/2001GL013714, 140–3.
Debreu, L., Marchesiello, P., Penven, P., Cambon, G., 2012. Two-way nesting in split-explicit ocean models: algorithms, implementation and validation. Ocean Model. 49 (50), 1–21. https://doi.org/10.1016/j.ocemod.2012.03.003.
Dee, D.P., de, Uppala, Simmons, Berrisford, Poli, P., Kobayashi, S., Andrae, U., Balmaseda, M., Balsamo, G., Bauer, Bechtold, Beljaars, Berg, van, Bidlot, J., Bormann, N., Delsol, Dragani, R., Fuentes, M., Vitart, F., 2011. The ERA-Interim reanalysis: configuration and performance of the data assimilation system. Q. J. R. Meteorol. Soc. 137, 553–597. https://doi.org/10.1002/qj.828.
Dray, S., Bauman, D., Blanchet, G., Borcard, D., Clappe, S., Guenard, G., Jombart, T., Larocque, G., Legendre, P., Madi, N., Wagner, H.H., 2022. Adespatial: Multivariate Multiscale Spatial Analysis. R Package Version 0.3-16.
Du Preez, C., Curtis, J.M.R., Clarke, M.E., 2016. The structure and distribution of benthic communities on a shallow seamount (cobb seamount, northeast pacific ocean). PLoS One 11, e0165513. https://doi.org/10.1371/journal.pone.0165513.
Dufrêne, M., Legendre, P., 1997. Species assemblages and indicator species: the need for a flexible asymmetrical approach. Ecol. Monogr. 67, 22.
Edler, D., Guedes, T., Zizka, A., Rosvall, M., Antonelli, A., 2016. Infomap bioregions: interactive mapping of biogeographical regions from species distributions. Syst Biol syw087. https://doi.org/10.1093/sysbio/syw087.
Fairall, C., Bradley, E., Rogers, D., Edson, J., Young, G., 1996. Bulk parameterization of air-sea fluxes for the Tropical Ocean Global Atmosphere Coupled Ocean-Atmosphere Response Experiment (TOGA-COARE). J. Geophys. Res. 101, 3747–3764. https://doi.org/10.1029/95JC03205.
Faivre, L., Teichert, N., Valade, P., Monnier, O., Couprie, S., 2020. Evaluation des conditions de référence des cours d'eau de Mayotte - projet REZORD -MAY - volet 1 : caractérisation des pressions s'exerçant sur les populations de Poissons et de macro-crustacés amphihalins de Mayotte. Rapport final OCE, MNHN, OFB.
Ferry, N., Parent, L., Garric, G., Bricaud, C., Testut, C.E., Le Galloudec, O., Lellouche, J.-M., Drevillon, M., Greiner, E., Barnier, B., Molines, J.-M., Jourdain, N.C., Guinehut, S., Cabanes, C., Zawadzki, L., 2012. GLORYS2V1 global ocean reanalysis of the altimetric era (1992-2009) at meso scale. Mercator Ocean Quaterly Newsletter 29–39.
FAO species identification sheets for fishery purposes. In: Fischer, W., Bianchi, G. (Eds.), 1984. Western Indian Ocean (Fishing Area 51), Prepared and Printed with the Support of the Danish International Development Agency (DANIDA). FAO, Rome.
Genin, A., Dayton, P.K., Lonsdale, P.F., Spiess, F.N., 1986. Corals on seamount peaks provide evidence of current acceleration over deep-sea topography. Nature 322, 59–61. https://doi.org/10.1038/322059a0.
Giusti, M., Innocenti, C., Canese, S., 2014. Predicting suitable habitat for the gold coral savalia savaglia (bertoloni, 1819) (Cnidaria, Zoantharia) in the South tyrrhenian sea. Continent. Shelf Res. 81, 19–28. https://doi.org/10.1016/j.csr.2014.03.011.
Goode, S.L., Rowden, A.A., Bowden, D.A., Clark, M.R., Stephenson, F., 2021. Fine-scale mapping of mega-epibenthic communities and their patch characteristics on two New Zealand seamounts. Front. Mar. Sci. 8, 765407 https://doi.org/10.3389/fmars.2021.765407.
Grassle, J.F., Sanders, H.L., Hessler, R.R., Rowe, G.T., McLellan, T., 1975. Pattern and zonation: a study of the bathyal megafauna using the research submersible Alvin. Deep Sea Research and Oceanographic Abstracts 22, 457–481. https://doi.org/10.1016/0011-7471(75)90020-0.
Hall-Spencer, J., Rogers, A., Davies, J., Foggo, A., 2007. Deep-sea Coral Distribution on Seamounts, Oceanic Islands, and Continental Slopes in the Northeast Atlantic 13.
Hanafi-Portier, M., Samadi, S., Cárdenas, P., Pante, E. Image-based Ecological Assessment of Deep-Sea Cnidarian and Sponge Assemblages through a Morpho-Functional Approach (Unpublished results).
Hanafi-Portier, M., Samadi, S., Corbari, L., Chan, T.-Y., Chen, W.-J., Chen, J.-N., Lee, M.-Y., Mah, C., Saucède, T., Borremans, C., Olu, K., 2021. When imagery and physical sampling work together: toward an integrative methodology of deep-sea image-based megafauna identification. Front. Mar. Sci. 8, 749078 https://doi.org/10.3389/fmars.2021.749078.
Hancke, L., Roberts, M.J., Ternon, J.F., 2014. Surface drifter trajectories highlight flow pathways in the Mozambique Channel. Deep Sea Res. Part II Top. Stud. Oceanogr. 100, 27–37. https://doi.org/10.1016/j.dsr2.2013.10.014.
Hein, J.R., Conrad, T.A., Staudigel, H., 2010. Seamount mineral deposits, a source of rare metals for high-technology industries. Oceanography 23, 184–189.
Henry, L.-A., Vad, J., Findlay, H.S., Murillo, J., Milligan, R., Roberts, J.M., 2015. Environmental variability and biodiversity of megabenthos on the hebrides terrace seamount (northeast atlantic). Sci. Rep. 4 https://doi.org/10.1038/srep05589.
Hsieh, T.C., Ma, K.H., Chao, A., 2020. iNEXT: iNterpolation and EXTrapolation for Species Diversity. R package version 2.0.20.
Jorry, S., 2014. PTOLEMEE Cruise, RV L'Atalante. https://doi.org/10.17600/14000900.
Jorry, S.J., Jouet, G., Edinger, E.N., Toucanne, S., Counts, J.W., Miramontes, E., Courgeon, S., Riveiros, N.V., Le Roy, P., Camoin, G.F., 2020. From platform top to adjacent deep sea: new source-to-sink insights into carbonate sediment production and transfer in the SW Indian Ocean (Glorieuses archipelago). Mar. Geol. 423, 106144 https://doi.org/10.1016/j.margeo.2020.106144.
Jouet, G., Deville, E., 2015. PAMELA-MOZ04 Cruise, RV Pourquoi Pas ? https://doi.org/10.17600/15000700.
Kaufmann, R.S., Wakefield, W.W., Genin, A., 1989. Distribution of epibenthic megafauna and lebensspuren on two central North Pacific seamounts. Deep Sea Research Part A. Oceanographic Research Papers 36, 1863–1896. https://doi.org/10.1016/0198-0149(89)90116-7.
Kvile, K.Ø., Taranto, G.H., Pitcher, T.J., Morato, T., 2014. A global assessment of seamount ecosystems knowledge using an ecosystem evaluation framework. Biol. Conserv. 173, 108–120. https://doi.org/10.1016/j.biocon.2013.10.002.
Langa, A.Á.A., 2021. Seasonal and spatial variability of primary production in the Mozambique channel. WROS 10, 61. https://doi.org/10.11648/j.wros.20211003.14.
Langenkämper, D., Zurowietz, M., Schoening, T., Nattkemper, T.W., 2017. Biigle 2.0 - browsing and annotating large marine image collections. Front. Mar. Sci. 4 https://doi.org/10.3389/fmars.2017.00083.
Lapointe, A.E., Watling, L., France, S.C., Auster, P.J., 2020. Megabenthic assemblages in the lower bathyal (700–3000 m) on the new england and corner rise seamounts, northwest atlantic. Deep Sea Res. Oceanogr. Res. Pap. 165, 103366 https://doi.org/10.1016/j.dsr.2020.103366.

Lawrence, J.M., Jangoux, M., 2020. Chapter 21: cidaroids. In: Lawrence, J.M. (Ed.), Sea Urchins: Biology and Ecology.
Legendre, P., 2014. Interpreting the replacement and richness difference components of beta diversity: replacement and richness difference components. Global Ecol. Biogeogr. 23, 1324–1334. https://doi.org/10.1111/geb.12207.
Legendre, P., De Cáceres, M., 2013. Beta diversity as the variance of community data: dissimilarity coefficients and partitioning. Ecol. Lett. 16, 951–963. https://doi.org/10.1111/ele.12141.
Legendre, P., Gallagher, E.D., 2001. Ecologically meaningful transformations for ordination of species data. Oecologia 129, 271–280. https://doi.org/10.1007/s004420100716.
Legendre, P., Legendre, L.F., 2012. Numerical Ecology, third ed. Elsevier.
Leroy, B., 2022. Biogeonetworks: Biogeographical Network Manipulation and Analysis. R Package Version 0.1.2.
Leroy, B., Dias, M.S., Giraud, E., Hugueny, B., Jézéquel, C., Leprieur, F., Oberdorff, T., Tedesco, P.A., 2019. Global biogeographical regions of freshwater fish species. J. Biogeogr. 46, 2407–2419. https://doi.org/10.1111/jbi.13674.
Lévy, M., Klein, P., Treguier, A.-M., 2001. Impact of sub-mesoscale physics on production and subduction of phytoplankton in an oligotrophic regime. J. Mar. Res. 59, 535–565. https://doi.org/10.1357/002224001762842181.
Lima, M.J., Sala, I., Caldeira, R.M.A., 2020. Physical connectivity between the NE atlantic seamounts. Front. Mar. Sci. 7, 238. https://doi.org/10.3389/fmars.2020.00238.
Long, D.J., Baco, A.R., 2014. Rapid change with depth in megabenthic structure-forming communities of the Makapu'u deep-sea coral bed. Deep Sea Res. Part II Top. Stud. Oceanogr. 99, 158–168. https://doi.org/10.1016/j.dsr2.2013.05.032.
Lundsten, L., Barry, J., Cailliet, G., Clague, D., DeVogelaere, A., Geller, J., 2009. Benthic invertebrate communities on three seamounts off southern and central California, USA. Mar. Ecol. Prog. Ser. 374, 23–32. https://doi.org/10.3354/meps07745.
Lundsten, L., DeVogelaere, A., Barry, J., Clague, D., 2006. A Characterization of the Megafauna on Davidson Seamount, vol. 1. AGU Fall Meeting Abstracts, 0650.
Macpherson, E., Richer De Forges, B., Schnabel, K., Samadi, S., Boisselier, M.-C., Garcia-Rubies, A., 2010. Biogeography of the deep-sea galatheid squat lobsters of the Pacific Ocean. Deep Sea Res. Oceanogr. Res. Pap. 57, 228–238. https://doi.org/10.1016/j.dsr.2009.11.002.
Malauene, B.S., Shillington, F.A., Roberts, M.J., Moloney, C.L., 2014. Cool, elevated chlorophyll-a waters off northern Mozambique. Deep Sea Res. Part II Top. Stud. Oceanogr. 100, 68–78. https://doi.org/10.1016/j.dsr2.2013.10.017.
Marsac, F., Barlow, R., Ternon, J.F., Ménard, F., Roberts, M., 2014. Ecosystem functioning in the Mozambique Channel: synthesis and future research. Deep Sea Res. Part II Top. Stud. Oceanogr. 100, 212–220. https://doi.org/10.1016/j.dsr2.2013.10.028.
Maureaud, A.A., Reygondeau, G., Ingenloff, K., Vigneron, J.G., Watling, L., Winner, K., Jetz, W., 2023. A global biogeographic regionalization of the benthic ocean (preprint). Open Science Framework. https://doi.org/10.31219/osf.io/nkjvf.
McClain, C.R., Lundsten, L., Barry, J., DeVogelaere, A., 2010. Assemblage structure, but not diversity or density, change with depth on a northeast Pacific seamount: bathymetric patterns in diversity, abundance and assemblage structure. Mar. Ecol. 31, 14–25. https://doi.org/10.1111/j.1439-0485.2010.00367.x.
McClain, C.R., Lundsten, L., Ream, M., Barry, J., DeVogelaere, A., 2009. Endemicity, biogeography, composition, and community structure on a northeast pacific seamount. PLoS One 4, e4141. https://doi.org/10.1371/journal.pone.0004141.
Mecho, A., Easton, E.E., Sellanes, J., Gorny, M., Mah, C., 2019. Unexplored diversity of the mesophotic echinoderm fauna of the Easter Island ecoregion. Mar Biol 166, 91. https://doi.org/10.1007/s00227-019-3537-x.
Miller, K., Gunasekera, R., 2017. A comparison of genetic connectivity in two deep sea corals to examine whether seamounts are isolated islands or stepping stones for dispersal. Sci. Rep. 7, 46103 https://doi.org/10.1038/srep46103.
Miller, K., Williams, A., Rowden, A.A., Knowles, C., Dunshea, G., 2010. Conflicting estimates of connectivity among deep-sea coral populations: connectivity among deep-sea coral populations. Mar. Ecol. 31, 144–157. https://doi.org/10.1111/j.1439-0485.2010.00380.x.
Miramontes, E., Jorry, S.J., Jouet, G., Counts, J.W., Courgeon, S., Le Roy, P., Guerin, C., Hernández-Molina, F.J., 2019a. Deep-water dunes on drowned isolated carbonate terraces (Mozambique Channel, south-west Indian Ocean). Sedimentology 66, 1222–1242. https://doi.org/10.1111/sed.12572.
Miramontes, E., Penven, P., Fierens, R., Droz, L., Toucanne, S., Jorry, S.J., Jouet, G., Pastor, L., Silva Jacinto, R., Gaillot, A., Giraudeau, J., Raisson, F., 2019b. The influence of bottom currents on the Zambezi Valley morphology (Mozambique Channel, SW Indian Ocean): in situ current observations and hydrodynamic modelling. Mar. Geol. 410, 42–55. https://doi.org/10.1016/j.margeo.2019.01.002.
Miyamoto, M., Kiyota, M., 2017. Application of association analysis for identifing indicator taxa of vulnerable marine ecosystems in the Emperor Seamounts area, North Pacific Ocean. Ecol. Indicat. 78, 301–310. https://doi.org/10.1016/j.ecolind.2017.03.028.
Miyamoto, M., Kiyota, M., Hayashibara, T., Nonaka, M., Imahara, Y., Tachikawa, H., 2017. Megafaunal composition of cold-water corals and other deep-sea benthos in the southern Emperor Seamounts area, North Pacific Ocean. Galaxea. Journal of Coral Reef Studies 19, 19–30. https://doi.org/10.3755/galaxea.19.1_19.
Morato, T., Clark, M.R., 2007. Seamount fishes: ecology and life histories. In: Pitcher, T. J., Morato, T., Paul, J.B.H., Clark, M.R., Nigel, H., Ricardo, S.S. (Eds.), Seamounts: Ecology, Fisheries & Conservation. John Wiley & Sons, Ltd, pp. 170–188. https://doi.org/10.1002/9780470691953.ch9.
Morato, T., Hoyle, S.D., Allain, V., Nicol, S.J., 2010. Seamounts are hotspots of pelagic biodiversity in the open ocean. Proc. Natl. Acad. Sci. U.S.A. 107, 9707–9711. https://doi.org/10.1073/pnas.0910290107.
Morato, T., Varkey, D., Damaso, C., Machete, M., Santos, M., Prieto, R., Pitcher, T., Santos, R., 2008. Evidence of a seamount effect on aggregating visitors. Mar. Ecol. Prog. Ser. 357, 23–32. https://doi.org/10.3354/meps07269.
Morgan, N.B., Cairns, S., Reiswig, H., Baco, A.R., 2015. Benthic megafaunal community structure of cobalt-rich manganese crusts on Necker Ridge. Deep Sea Res. Oceanogr. Res. Pap. 104, 92–105. https://doi.org/10.1016/j.dsr.2015.07.003.
Morgan, N.B., Goode, S., Roark, E.B., Baco, A.R., 2019. Fine scale assemblage structure of benthic invertebrate megafauna on the north pacific seamount mokumanamana. Front. Mar. Sci. 6, 715. https://doi.org/10.3389/fmars.2019.00715.
Narayanaswamy, B.E., Hughes, D.J., Howell, K.L., Davies, J., Jacobs, C., 2013. First observations of megafaunal communities inhabiting george bligh bank, northeast atlantic. Deep Sea Res. Part II Top. Stud. Oceanogr. 92, 79–86. https://doi.org/10.1016/j.dsr2.2013.03.004.
Obura, D., Church, J., Gabrié, C., Macharia, D., 2012. Assessing Marine World Heritage from an Ecosystem Perspective. The Western Indian Ocean 125.
O'Hara, T., 2008. Bioregionalisation of the Waters Around Lord Howe and Norfolk Islands Using Brittle Stars (Echinodermata: Ophiuroidea).
O'Hara, T.D., 2007. Seamounts: centres of endemism or species richness for ophiuroids? Global Ecol. Biogeogr. 16, 720–732. https://doi.org/10.1111/j.1466-8238.2007.00329.x.
O'Hara, T.D., Consalvey, M., Lavrado, H.P., Stocks, K.I., 2010. Environmental predictors and turnover of biota along a seamount chain: assemblage composition along a seamount chain. Mar. Ecol. 31, 84–94. https://doi.org/10.1111/j.1439-0485.2010.00379.x.
O'Hara, T.D., Rowden, A.A., Williams, A., 2008. Cold-water coral habitats on seamounts: do they have a specialist fauna? Divers. Distrib. 14, 925–934. https://doi.org/10.1111/j.1472-4642.2008.00495.x.
O'Hara, T.D., Tittensor, D.P., 2010. Environmental drivers of ophiuroid species richness on seamounts: ophiuroid seamount species richness. Mar. Ecol. 31, 26–38. https://doi.org/10.1111/j.1439-0485.2010.00373.x.
Oksanen, J., Blanchet, F.G., Friendly, M., Kindt, R., Legendre, P., McGlinn, D., Minchin, P.R., O'Hara, R.B., Gavin, L.S., Peter, S., Stevens, H., henry, M., Szoecs, E., Wagner, H., 2020. Vegan: Community Ecology Package. R Package Version 2, pp. 5–7.
Olu, K., 2014. PAMELA-MOZ01 Cruise. RV L'Atalante. https://doi.org/10.17600/14001000.
Pante, E., France, S.C., Gey, D., Cruaud, C., Samadi, S., 2015. An inter-ocean comparison of coral endemism on seamounts: the case of *Chrysogorgia*. J. Biogeogr. 42, 1907–1918. https://doi.org/10.1111/jbi.12564.
Peres-Neto, P.R., Legendre, P., 2010. Estimating and controlling for spatial structure in the study of ecological communities. Global Ecol. Biogeogr. 19, 174–184. https://doi.org/10.1111/j.1466-8238.2009.00506.x.
Piepenburg, D., Müller, B., 2004. Distribution of epibenthic communities on the great meteor seamount (North-east atlantic) mirrors pelagic processes. Arch. Fish. Mar. Res. 17.
Puerta, P., Mosquera-Giménez, Á., Reñones, O., Domínguez-Carrió, C., Rueda, J.L., Urra, J., Carreiro-Silva, M., Blasco-Ferre, J., Santana, Y., Gutiérrez-Zárate, C., Vélez-Belchí, P., Rivera, J., Morato, T., Orejas, C., 2022. Variability of deep-sea megabenthic assemblages along the western pathway of the Mediterranean outflow water. Deep Sea Res. Oceanogr. Res. Pap. 185, 103791 https://doi.org/10.1016/j.dsr.2022.103791.
R Core Team, 2021. R: A Language and Environment for Statistical Computing. R Foundation for Statistical Computing, Vienna.
Ramos, M., Bertocci, I., Tempera, F., Calado, G., Albuquerque, M., Duarte, P., 2016. Patterns in megabenthic assemblages on a seamount summit (ormonde peak, gorringe bank, northeast atlantic). Mar. Ecol. 37, 1057–1072. https://doi.org/10.1111/maec.12353.
Roberts, D.W., 2019. Labdsv: Ordination and Multivariate Analysis for Ecology. R Package Version 2.0-1.
Rogers, A.D., 2018. The biology of seamounts: 25 Years on. In: Advances in Marine Biology. Elsevier, pp. 137–224. https://doi.org/10.1016/bs.amb.2018.06.001.
Rojas, A., Patarroyo, P., Mao, L., Bengtson, P., Kowalewski, M., 2017. Global biogeography of Albian ammonoids: a network-based approach. Geology 45, 659–662. https://doi.org/10.1130/G38944.1.
Rowden, A.A., Dower, J.F., Schlacher, T.A., Consalvey, M., Clark, M.R., 2010a. Paradigms in seamount ecology: fact, fiction and future: paradigms in seamount ecology. Mar. Ecol. 31, 226–241. https://doi.org/10.1111/j.1439-0485.2010.00400.x.
Rowden, A.A., Schlacher, T.A., Williams, A., Clark, M.R., Stewart, R., Althaus, F., Bowden, D.A., Consalvey, M., Robinson, W., Dowdney, J., 2010b. A test of the seamount oasis hypothesis: seamounts support higher epibenthic megafaunal biomass than adjacent slopes: a test of the seamount oasis hypothesis. Mar. Ecol. 31, 95–106. https://doi.org/10.1111/j.1439-0485.2010.00369.x.
Rowden, A.A., Schnabel, K.E., Schlacher, T.A., Macpherson, E., Ahyong, S.T., Richer de Forges, B., 2010c. Squat lobster assemblages on seamounts differ from some, but not all, deep-sea habitats of comparable depth: squat lobster assemblages of deep-sea habits. Mar. Ecol. 31, 63–83. https://doi.org/10.1111/j.1439-0485.2010.00374.x.
Sautya, S., Ingole, B., Ray, D., Stöhr, S., Samudrala, K., Raju, K.A.K., Mudholkar, A., 2011. Megafaunal community structure of andaman seamounts including the back-arc basin – a quantitative exploration from the Indian ocean. PLoS One 6, e16162. https://doi.org/10.1371/journal.pone.0016162.
Schlacher, T.A., Baco, A.R., Rowden, A.A., O'Hara, T.D., Clark, M.R., Kelley, C., Dower, J.F., 2014. Seamount benthos in a cobalt-rich crust region of the central Pacific: conservation challenges for future seabed mining. Divers. Distrib. 20, 491–502. https://doi.org/10.1111/ddi.12142.

Schönberg, C.H.L., 2021. No taxonomy needed: sponge functional morphologies inform about environmental conditions. Ecol. Indicat. 129. DDdoi.orgD10.101BDj.ecolind.2021.107A0B.
Shchepetkin, A.F., McWilliams, J.C., 2005. The regional oceanic modeling system (ROMS): a split-explicit, free-surface, topography-following-coordinate oceanic model. Ocean Model. 9, 347–404. https://doi.org/10.1016/j.ocemod.2004.08.002.
Shen, C., Lu, B., Li, Z., Zhang, R., Chen, W., Xu, P., Yao, H., Chen, Z., Pang, J., Wang, C., Zhang, D., 2021. Community structure of benthic megafauna on a seamount with cobalt-rich ferromanganese crusts in the northwestern Pacific Ocean. Deep Sea Res. Oceanogr. Res. Pap. 178, 103661 https://doi.org/10.1016/j.dsr.2021.103661.
Standaert, W., Puerta, P., Mastrototaro, F., Palomino, D., Aguilar, R., Ramiro-Sánchez, B., Vázquez, J.-T., Guillamón, O.S., Marin, P., Blanco, J., Orejas, C., 2023. Habitat suitability models of a critically endangered cold-water coral, isidella elongata. In: The Mallorca Channel. Thalassas. https://doi.org/10.1007/s41208-023-00531-y.
Starr, R., Cortés, J., Barnes, C., Green, K., Breedy, O., 2012. Characterization of deepwater invertebrates at Isla del Coco National Park and Las Gemelas Seamount, Costa Rica. Rev. Biol. Trop. 60, 303–319. https://doi.org/10.15517/rbt.v60i3.28406.
Stashchuk, N., Vlasenko, V., 2021. Internal wave dynamics over isolated seamount and its influence on coral larvae dispersion. Front. Mar. Sci. 8.
Staudigel, H., Clague, D.A., 2010. The geological history of deep-sea volcanoes: biosphere, hydrosphere, and lithosphere interactions. Oceanography 23, 58–71. https://doi.org/10.5670/oceanog.2010.62.
Stöhr, S., O'Hara, T.D., Thuy, B., 2012. Global diversity of brittle stars (echinodermata: Ophiuroidea). PLoS One 7, e31940. https://doi.org/10.1371/journal.pone.0031940.
Stratmann, T., Simon-Lledó, E., Morganti, T.M., de Kluijver, A., Vedenin, A., Purser, A., 2022. Habitat types and megabenthos composition from three sponge-dominated high-Arctic seamounts. Sci. Rep. 12, 20610 https://doi.org/10.1038/s41598-022-25240-z.
Tapia-Guerra, J.M., Mecho, A., Easton, E.E., Gallardo, M. de los Á., Gorny, M., Sellanes, J., 2021. First description of deep benthic habitats and communities of oceanic islands and seamounts of the Nazca Desventuradas Marine Park, Chile. Sci. Rep. 11, 6209. https://doi.org/10.1038/s41598-021-85516-8.
Tew-Kai, E., Marsac, F., 2009. Patterns of variability of sea surface chlorophyll in the Mozambique Channel: a quantitative approach. J. Mar. Syst. 77, 77–88. https://doi.org/10.1016/j.jmarsys.2008.11.007.
Thistle, D., 2003. The Deep-Sea Floor: an Overview. Ecosystems of the World. Book 28.
Thomassin, B., 1977. BENTHEDI I Cruise. RV Le Suroît. https://doi.org/10.17600/77003111.
Tittensor, D.P., Baco, A.R., Brewin, P.E., Clark, M.R., Consalvey, M., Hall-Spencer, J., Rowden, A.A., Schlacher, T., Stocks, K.I., Rogers, A.D., 2009. Predicting global habitat suitability for stony corals on seamounts. J. Biogeogr. 36, 1111–1128.
Victorero, L., Robert, K., Robinson, L.F., Taylor, M.L., Huvenne, V.A.I., 2018. Species replacement dominates megabenthos beta diversity in a remote seamount setting. Sci. Rep. 8 https://doi.org/10.1038/s41598-018-22296-8.
Vilhena, D.A., Antonelli, A., 2015. A network approach for identifying and delimiting biogeographical regions. Nat. Commun. 6, 6848. https://doi.org/10.1038/ncomms7848.
Walbridge, S., Slocum, Pobuda, Wright, D., 2018. Unified geomorphological analysis workflows with benthic terrain modeler. Geosciences 8, 94. https://doi.org/10.3390/geosciences8030094.
Watling, L., Auster, P.J., 2021. Vulnerable marine ecosystems, communities, and indicator species: confusing concepts for conservation of seamounts. Front. Mar. Sci. 8, 622586 https://doi.org/10.3389/fmars.2021.622586.
Watling, L., Guinotte, J., Clark, M.R., Smith, C.R., 2013. A proposed biogeography of the deep ocean floor. Prog. Oceanogr. 111, 91–112. https://doi.org/10.1016/j.pocean.2012.11.003.
Watling, L., Lapointe, A., 2022. Global biogeography of the lower bathyal (700–3000 m) as determined from the distributions of cnidarian anthozoans. Deep Sea Res. Oceanogr. Res. Pap. 181, 103703 https://doi.org/10.1016/j.dsr.2022.103703.
Weatherall, P., Marks, K.M., Jakobsson, M., Schmitt, T., Tani, S., Arndt, J.E., Rovere, M., Chayes, D., Ferrini, V., Wigley, R., 2015. A new digital bathymetric model of the world's oceans. Earth Space Sci. 2, 331–345. https://doi.org/10.1002/2015EA000107.
White, M., Bashmachnikov, I., Arístegui, J., Martins, A., 2007. Physical processes and seamount productivity. In: Pitcher, T.J., Morato, T., Hart, P.J.B., Clark, M.R., Haggan, N., Santos, R.S. (Eds.), Seamounts: Ecology, Conservation and Management, Fish and Aquatic Resources. Blackwell, Oxford, UK, pp. 65–84.
Wickham, H., Chang, W., Wickham, M.H., 2016. Package 'ggplot2'. Create elegant data visualisations using the grammar of graphics. Versiones 2 (1), 1–189.
Williams, A., Althaus, F., Clark, M.R., Gowlett-Holmes, K., 2011. Composition and distribution of deep-sea benthic invertebrate megafauna on the lord howe rise and norfolk ridge, southwest Pacific ocean. Deep Sea Res. Part II Top. Stud. Oceanogr. 58, 948–958. https://doi.org/10.1016/j.dsr2.2010.10.050.
Wilson, M.F.J., O'Connell, B., Brown, C., Guinan, J.C., Grehan, A.J., 2007. Multiscale terrain analysis of multibeam bathymetry data for habitat mapping on the continental slope. Mar. Geodesy 30, 3–35. https://doi.org/10.1080/01490410701295962.